



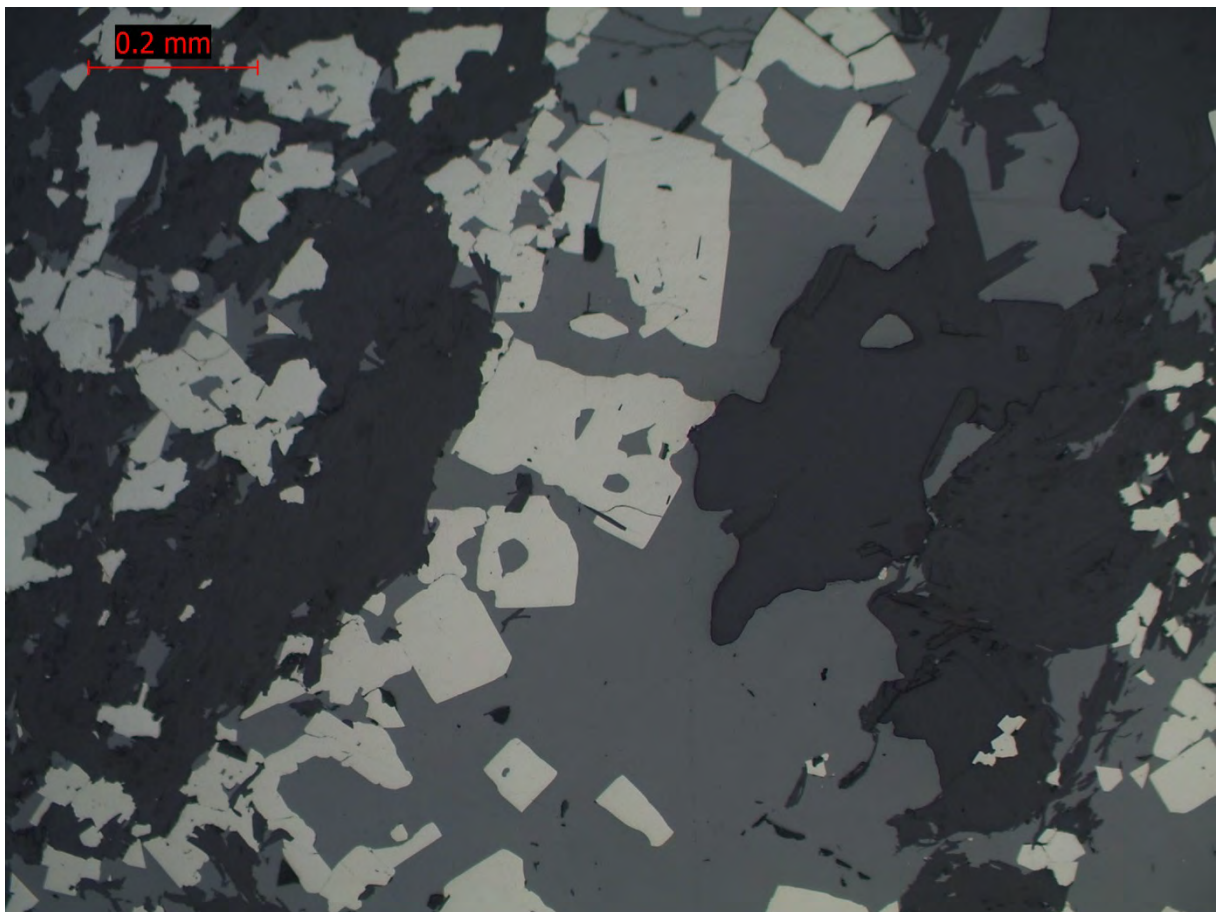
Stockholm
University

Bachelor Thesis

Degree Project in
Geology 15 hp

Sulfide paragenesis from the Renström Zn-Cu VMS deposit, Skellefte district Sweden

Stefan Franzén



Stockholm 2015

Department of Geological Sciences
Stockholm University
SE-106 91 Stockholm

Abstract

The aim of this project is to investigate the paragenesis of sulphide minerals in a series of drill core samples from the Renström Zn-Cu volcanogenic massive sulphide (VMS) deposit in the Skellefte district. A representative suite of 13 samples were chosen from different parts of drill core 2559 to create a cross section of the mineral deposit. These samples were examined with the help of both optical microscope and scanning electron microscope (SEM) to determine the paragenesis of the ore minerals as well as the effect of deformation and metamorphism on the mineralogy in the core.

The Renström mine VMS deposit, like many in the Skellefte district is considered to have formed at or near the seafloor during a period of active rifting and volcanism in the Paleoproterozoic. The area underwent considerable deformation and metamorphism after its original formation, and these processes have caused considerable recrystallization of the ore. The paragenesis of the ore minerals started with the formation of pyrite and arsenopyrite. Sphalerite, galena and tetrahedrite formed during the next phase and after that the first stage of chalcopyrite and pyrrhotite formed. The minerals were then remobilized through metamorphism and deformation caused by shearing. During the last mineral phase late stage chalcopyrite and pyrrhotite formed as well as various Ag-Sb sulfosalts. The outside of the ore zone which consists mostly of host rock seem to be the most deformed while the inside of the ore zone is less affected. This is most likely because the sulphide was recrystallized in response to deformation and metamorphism.

Contents

Abstract.....	2
Introduction.....	4
Geological setting.....	5
VMS deposits	6
Methods.....	7
Microscopy	7
SEM	7
Sampling	8
Results.....	10
Sample descriptions.....	10
SEM data	28
Discussion	38
Conclusion	40
Acknowledgements.....	40
References.....	41

Introduction

The demand for metals is increasing and better understanding of ore deposits is vital to find new sources to meet future needs. Mining of metal ore in Sweden has been active for thousands of years. One of the biggest and most important mining districts in Sweden is the Skellefte district (Fig.1). The Skellefte district occurs in an Early Proterozoic 1.90-1.87 Ga sedimentary and volcanic province of low to medium metamorphic grade in the Baltic Shield in northern Sweden. There are over 85 pyritic Zn-Cu-Au-Ag volcanogenic massive sulfide (VMS) deposits in the district as well as a small number of vein-hosted Au deposits and subeconomic porphyry Cu-Au-Mo deposits (Allen *et al.* 1996). Five of these deposits are in operation today and 21 deposits have been mined since 1924. Two interesting features of the Skellefte district are that many massive sulfide deposits are generally Au-rich and that all deposits have been metamorphosed.

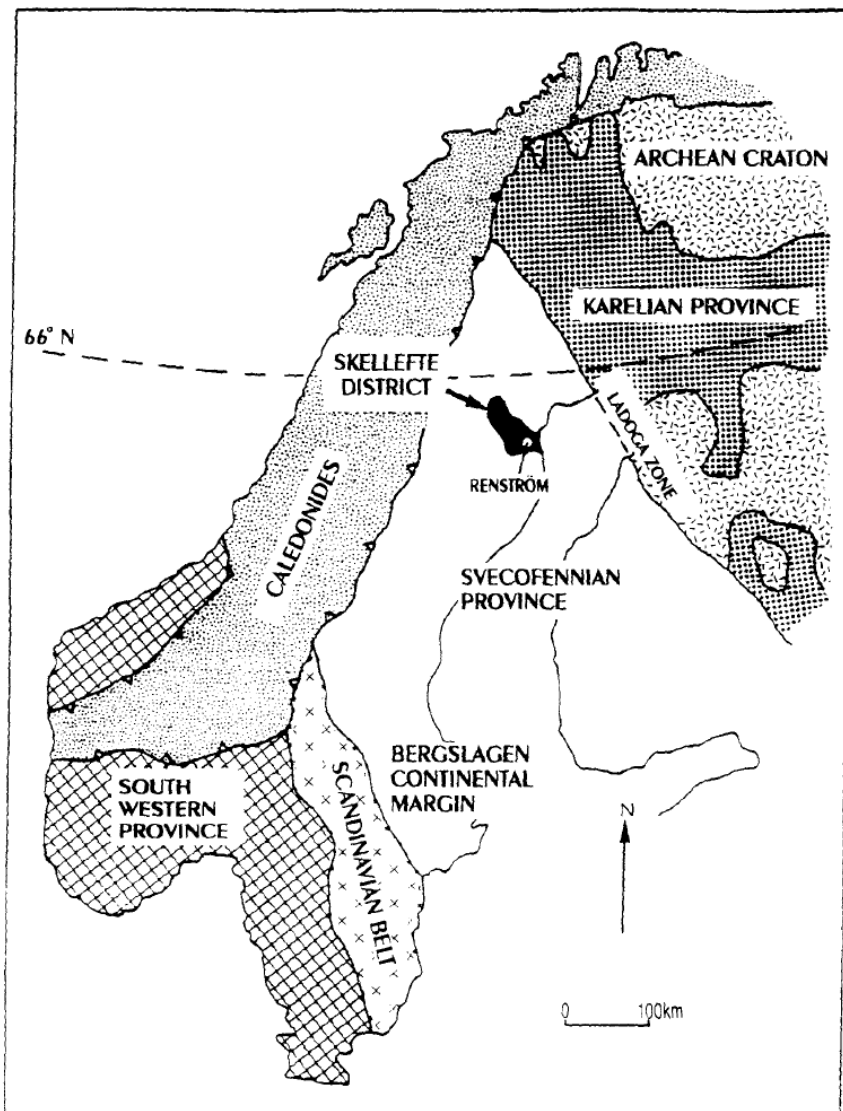


Fig.1. Terrane map of northern Scandinavia and Finland showing the location of the Skellefte district and the Renström deposit (Duckworth *et al.* 1993)

All of the deposits were deformed and metamorphosed during the main orogenic phase when the Skellefte district formed through collisions between continent and micro-continents during the Archean and Paleoproterozoic (2.06-1.78Ga). The metamorphic grade varies from greenschist facies in the center of the district to lower amphibolite facies to the west, south and east (*Allen et al. 1996*). Strong cleavage, stretching lineation and shearing are common and the ores have been variably recrystallized. The ores are interpreted as pre-tectonic based on structural evidence. It's relatively uncommon for VMS deposits to be Au-rich but there are many such deposits in the Skellefte district. The reason for this is unclear but one theory suggests that some of the more Au-rich deposits are submarine epithermal deposits rather than VMS deposits (*Allen et al. 1996*).

The Renström deposit is a Zn-Pb-Cu-Ag-Au VMS deposit located in the southern part of the Skellefte district. Like all massive sulfide deposits in the Skellefte district Renström was formed during the Early Proterozoic and is associated with volcanic units. One special feature of the Renström deposit is that it has undergone shearing which has resulted in the development of mylonitic fabrics within the sulphides (*Allen et al. 1996*). The massive sulfide ore is hosted in a shallow submarine to subaerial volcano-sedimentary sequence which has been metamorphosed and deformed.

The aim of this study is to investigate drill core 2559 from the Renström deposit and describe the mineralization and related alteration. The paragenesis of the drill core will also be determined using textural evidence. A key focus is to investigate the degree to which samples from the drill core have been altered and remobilized during metamorphism and deformation.

Geological setting

The Skellefte district is a part of the Fennoscandian Shield which formed during the Archean and Paleoproterozoic (2.06-1.78Ga) by rapid accretion of island arcs and several collisions between continents and micro-continents (*Weihed et al. 2005*). These collisions formed a complex array of orogens that were short-lived but intense involving voluminous magmatism. The Fennoscandian Shield forms the north-westernmost part of the East European craton and constitutes large parts of Finland, NW Russia, Norway, and Sweden. The oldest rocks found so far have been dated at 3.5 Ga and major orogeny's took place during the Archean and Paleoproterozoic (*Weihed et al. 2005*).

The Fennoscandian Shield hosts many economic mineral deposits but they are mainly restricted to the Paleoproterozoic parts of the shield although there are a few Archean deposits. The different types of deposits are: Ni-PGE deposits, orogenic gold deposits, VMS deposits, Fe-oxide deposits, iron oxide-copper-gold (IOCG) deposits, Cu-Au deposits and anorthosite-hosted Ti deposits (*Weihed et al. 2005*).

The massive sulfide deposits in the Skellefte district occur mainly in and along the top of a regional felsic-dominant volcanic unit attributed to a stage of intense, extensional, continental margin arc volcanism (*Weihed et al. 2005*). From facies analysis the paleogeography of this stage has been interpreted to be comprised of many scattered islands and shallow-water areas, surrounded by deeper seas (*Weihed et al. 2005*). All the major massive sulfide ores occur in below-wave base facies associations although some ores

occur close to above-wave base facies stratigraphic intervals and the summit of some volcanoes emerged above sea level.

There are 26 main volcanic, sedimentary, and intrusive facies in the Skellefte district. Through facies associations seven different volcano types have been defined in the district ranging from basaltic shields to andesite cones and rhyolite calderas (*Weihed et al. 2005*). Despite the many different types of volcanoes most massive sulfide ores are associated with just one volcano type: subaqueous rhyolite cryptodome-tuff volcanoes. These rhyolite volcanoes are 2 to 10 km in diameter, 250 to 1200 m thick at the center and are characterized by a small to moderate volume rhyolitic pyroclastic unit intruded by rhyolite cryptodomes, sills and dikes (*Weihed et al. 2005*).

VMS deposits

VMS deposits typically occur as lenses of polymetallic massive sulphide that form at or near the seafloor in submarine volcanic environments. They form from metal-enriched fluids associated with seafloor hydrothermal convection (*Galley et al. 2010*). The host rocks of VMS deposits can be either volcanic or sedimentary. VMS deposits are major sources of Zn, Cu, Pb, Ag and Au, and significant sources for Co, Sn, Se, Mn, Cd, In, Bi, Te, Ga and Ge. Some also contain significant amounts of As, Sb and Hg. Because VMS deposits are polymetallic they are one of the best deposits types for security against fluctuating prices of different metals (*Galley et al. 2010*).

VMS deposits forms at, or near, the seafloor through the focused discharge of hot, metal-rich hydrothermal fluids. For this reason, VMS deposits are classified under the general heading of "exhalative" deposits, which includes sedimentary exhalative (SEDEX) and sedimentary nickel deposits (*Galley et al. 2010*). Most VMS deposits have two components. The first component is a mound-shaped to tabular, stratabound body composed mostly of massive (>40%) sulphide, quartz and subordinate phyllosilicates and iron oxide minerals and altered silicate wallrock. This first component is typically underlain by the second component which is discordant to semi-concordant stockwork veins and disseminated sulphides. The stockwork vein systems, or "pipes", are enveloped in distinctive alteration halos, which may extend into the hanging-wall strata above the VMS deposit (*Galley et al. 2010*).

VMS deposits are grouped according to base metal content, Au content and host-rock lithology. VMS deposits are divided into Cu-Zn, Zn-Cu and Zn-Pb-Cu groups according to their contained ratios of these three metals. There is also a simple bimodal definition of "normal" vs. "Au-rich" VMS deposits (*Galley et al. 2010*). In the "Au-rich" vs. "normal" classification Au-rich VMS deposits are arbitrarily defined as those in which the concentrations of Au in ppm is greater than the combined base metals (Zn+Cu+Pb in wt. %). A third classification has five groups that indicate the dominant host-rock lithology. Host-rock lithologies include strata up to 3000m below the deposit and up to 5000m along strike. The five groups are mafic-dominated, bimodal mafic, bimodal-felsic, siliciclastic-mafic, and bimodal-siliciclastic (*Galley et al. 2010*). The order of this grouping reflects a progressive change from a less effusive to a more volcanoclastic-dominated environment as well as an increase in felsic volcanic rocks. These lithological groupings generally correlate with different tectonic settings. The groups associated with mafic volcanic and volcanoclastic strata are more common in oceanic arcs and spreading centers, whereas the two groups dominated by felsic

strata are more common in arc-continent margin and continental arc regimes (*Galley et al. 2010*).

The VMS deposits in the Skellefte district formed during the Early Proterozoic, 1.90-1.87 Ga, in an island arc either at or near the seafloor. Most of the massive sulfide ores in the Skellefte district are closely related to moderate size, marine, rhyolite cryptodome-tuff volcanoes rather than large pyroclastic caldera volcanoes, and it is believed that many ores formed by infiltration and replacement of subsea-floor strata rather than by exhalation on the sea floor (*Allen et al. 1996*).

Methods

Microscopy

Both reflected and transmitted light microscopy was used to examine thin sections from drill core 2559 and describe the mineralogy with a focus on the opaque ore minerals. Microscopy was also used to identify textures in order to determine the paragenesis of the ore minerals as well as the alteration and remobilization of the minerals caused by metamorphism and deformation.

SEM

Two thin sections (RS058 and RS073) were analyzed using a scanning electron microscope (SEM) to identify different ore minerals through chemical analysis and to take photographs of minerals and textures that are too small for optical microscopes.

The SEM uses a focused beam of electrons that gives a higher resolution than optical microscopes. SEM is capable of providing information on surface topography, crystalline structure, chemical composition of minerals and electrical behavior of the top 1 μm of the sample (*Vernon-Parry. 2000*).

Before the thin sections can be analyzed in the SEM they need to be coated with carbon to prevent the minerals from being charged by the electron beam which distorts the image. When the thin sections have been coated they can be placed inside the SEMs sample chamber on a specimen stub and air is pumped out of the chamber to create a vacuum. The signal from the electron beam is calibrated through use of a pure cobalt standard.

The SEM consists of an electron optical column, a vacuum system, electronics and software. The electron gun at the top of the column produces an electron beam that is focused into a fine spot as small as 1 nm in diameter on the sample surface. This beam is scanned in a rectangular raster over the sample and the surface of the sample emits electrons and x-rays as a response. These electrons and x-rays are picked up by detectors in the sample chamber and the intensities of these signals are measured and stored in computer memory. The stored values are then mapped as variations in brightness on the image display. Each element emits x-rays of a specific wavelength which makes it possible to determine the element and its quantity. The secondary electron (SE) signal is the most frequently used signal. It varies with the topography of the sample surface where edges are bright and recesses are dark. The ratio of the size of the displayed image to the size of the area scanned

on the sample gives the magnification. The model of the SEM used was a Quanta FEG 650.

Sampling

Drill core 2559 comes from the Simon ore lens in the Renström mine. The samples were chosen to represent a cross section of the drill core. Samples RS002 and RS018 represent the host rock above the ore lens. Samples RS034 to RS077 represent different sections of the ore lens. Samples RS081 and RS085 represent the host rock below the ore lens. A list of the different samples and their characteristics is provided in (Fig. 2).

Number	Depth	Lithology
2	23.5	Dacite
18	33.5	Pumice bearing volcanogenic sediment
34	41.5	Sphalerite-rich massive sulfide
38	44.15	Mixed massive sulfide
50	50.7	Mixed massive sulfide
53	52.1	Pyrite-rich massive sulfide
58	59.7	Sphalerite-rich massive sulfide
60	60.0	Mixed massive sulfide
69	64.3	Mixed massive sulfide
73	66.25	Pyrite-rich massive sulfide
77	68.85	Sphalerite-rich massive sulfide
81	70.8	Volcanogenic sediment
85	75.25	Pumice bearing volcanogenic sediment

Fig.2. List of samples including lithology and which depth they were taken from.

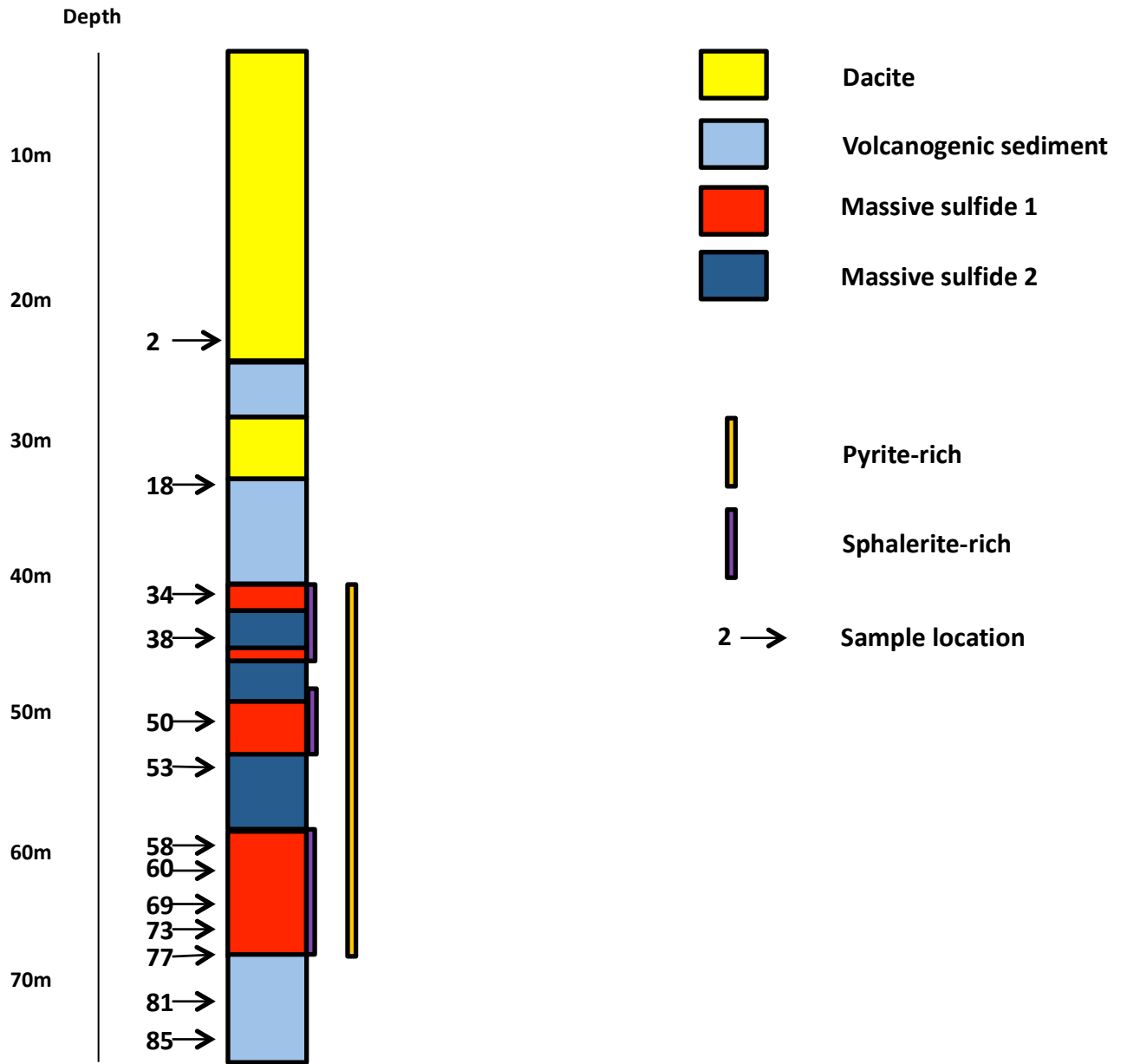


Fig.3. Core log of drill core 2559 showing depth, lithology and where the samples came from.

Results

Sample descriptions

RS002



Fig.4. Pyrite and ilmenite/titanite in a matrix of host rock.

Lithology: Dacite

Opaque minerals: Pyrite (<1 %), arsenopyrite (<1 %), pyrrhotite (<1 %) and ilmenite/titanite (<5 %).

Alteration minerals: Quartz, chlorite, biotite and carbonate.

Opaque mineralogy: Mostly host rock, some small pyrite and arsenopyrite cubes. Pyrite mostly occurs as euhedral cubes but sometimes as triangles or subhedral grains. The pyrrhotite occurs as subhedral grains. Skeletal ilmenite has been strongly replaced by titanite. The ilmenite/titanite is scattered throughout the sample as individual grains or small veins.

Alteration mineralogy: Quartz occurs as a matrix and there is on big inclusion/vein where carbonate and quartz have larger grain sizes. Chlorite and biotite occur as aggregates but chlorite also occurs as veins. There is a matrix of mainly quartz but also carbonate, chlorite

and biotite. All minerals also appear as clots and veins besides being part of the matrix. Some of the biotite is altering to titanite. A big carbonate vein crosscuts the sample and it is linked to a smaller quartz vein.

RS018

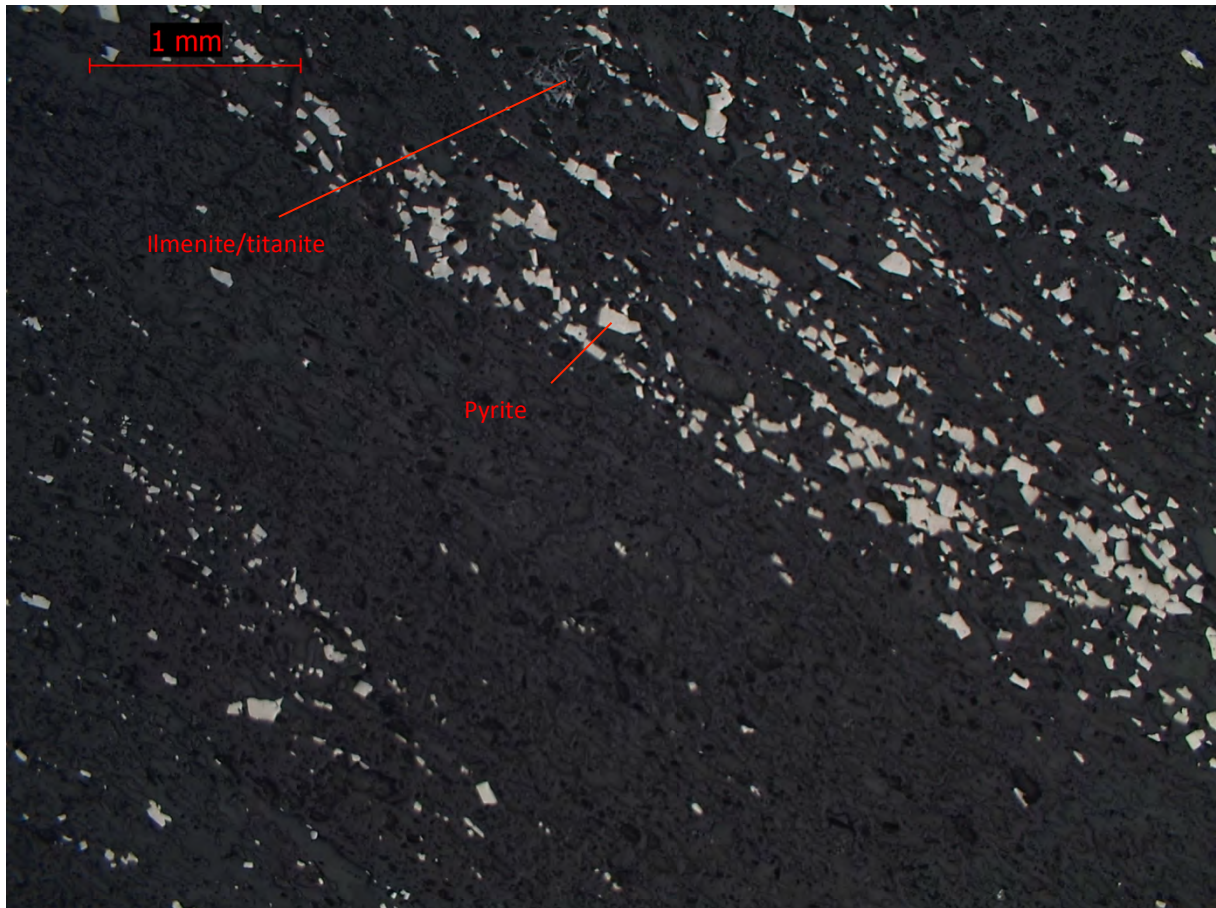


Fig.5. Layers of pyrite and host rock and a grain of ilmenite/titanite.

Lithology: Pumice bearing volcanogenic sediment

Opaque minerals: Pyrite (10 %), arsenopyrite (<5 %) and ilmenite/titanite (<1 %).

Alteration minerals: Quartz, muscovite, biotite and carbonate.

Opaque mineralogy: Heavily foliated sample with abundant pyrite and some arsenopyrite concentrated in certain areas and orientated in one direction because of the foliation creating alternating layers of pyrite/arsenopyrite, carbonate and mica. The pyrite is mostly euhedral with a few subhedral grains. The pyrite is relatively fine grained for the most part but some large aggregates exist. Skeletal ilmenite has been strongly replaced by titanite. The ilmenite/titanite is scattered throughout the sample as individual grains or small veins.

Alteration mineralogy: Biotite and muscovite occur together and forms layers of mica. There

is also some quartz associated with the carbonate layers. Carbonate is abundant and make up more than 50% of the sample. There are round fragments with pressure shadows on either side.

RS034

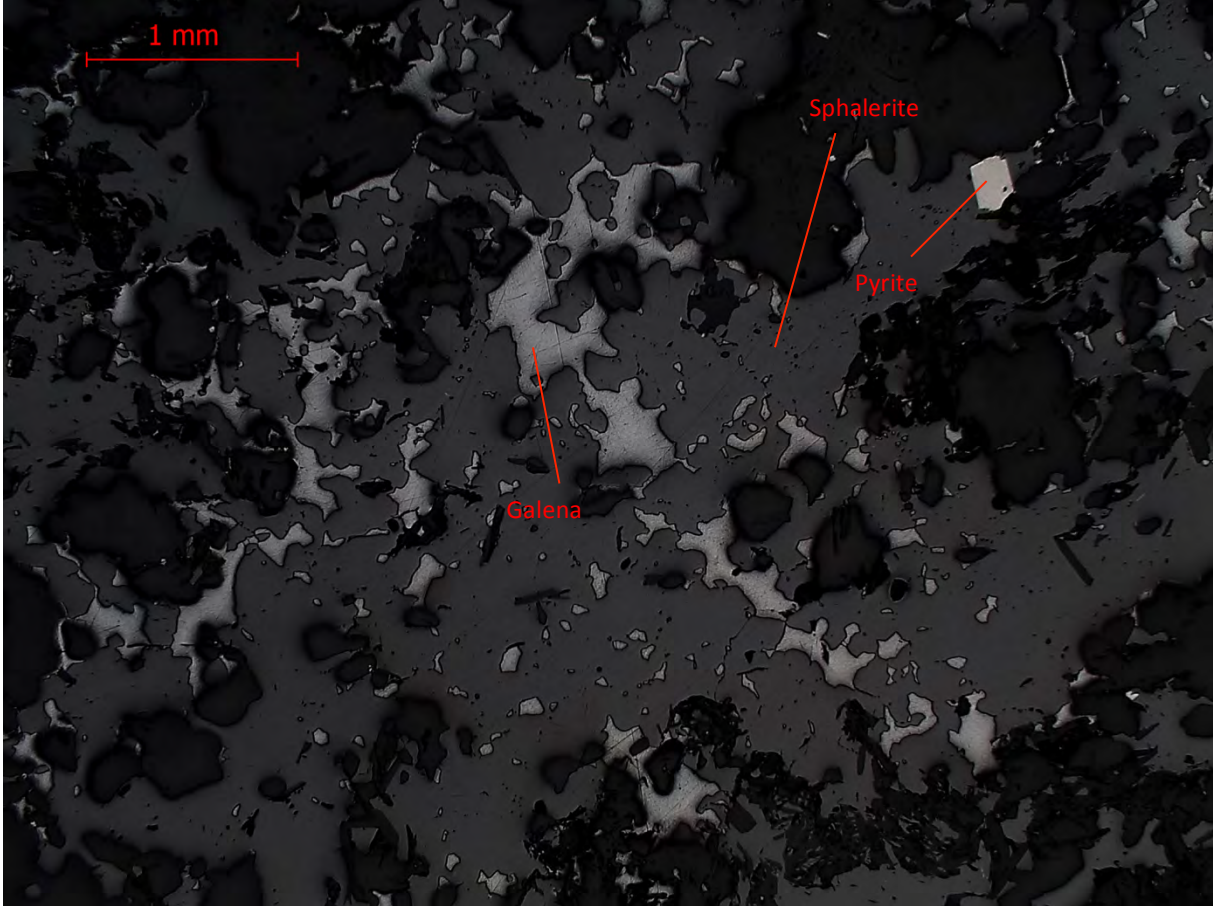


Fig.6. Patches of galena and a cube of pyrite in a matrix of sphalerite.

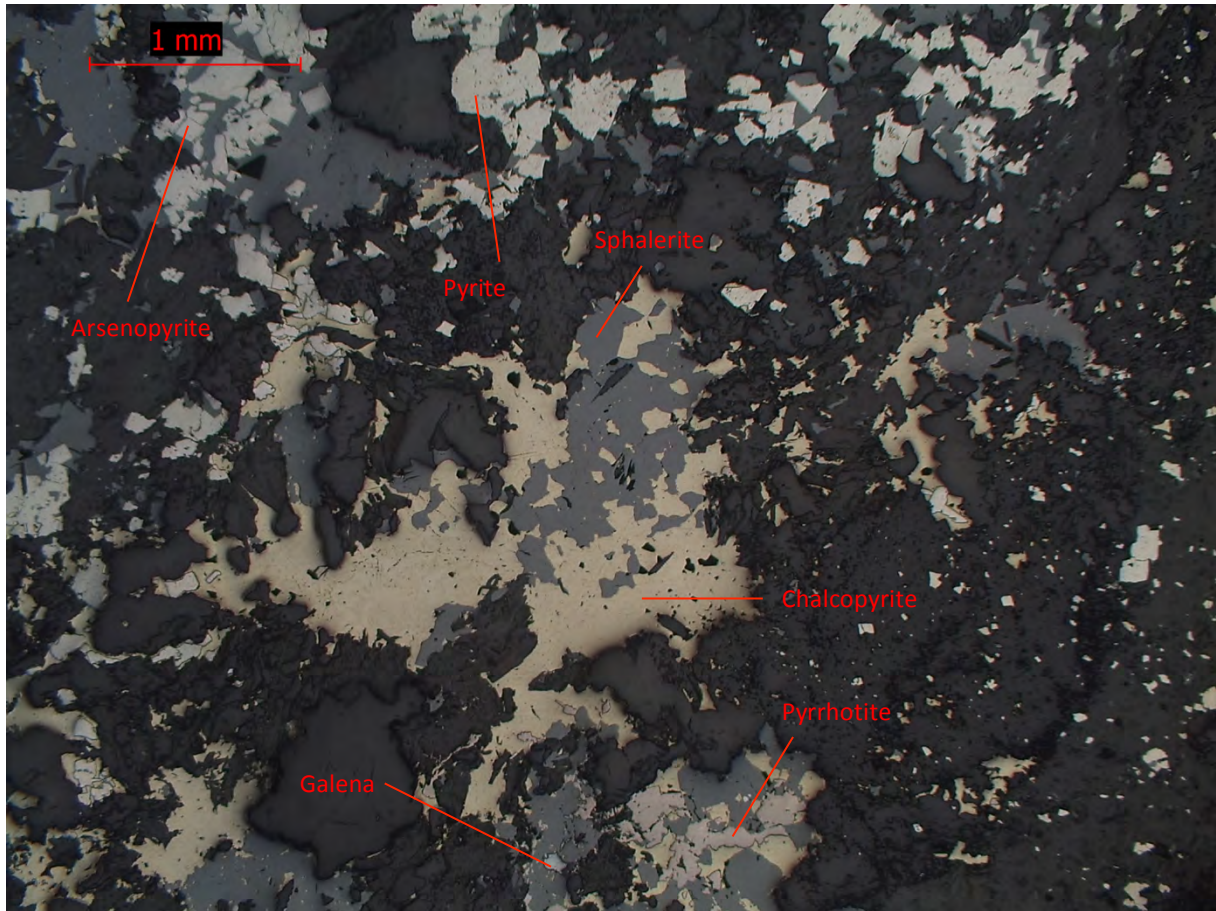


Fig.7. Patches of sphalerite, pyrite, chalcopyrite and pyrrhotite as well as some cubes of pyrite and arsenopyrite in a matrix of chlorite and carbonate.

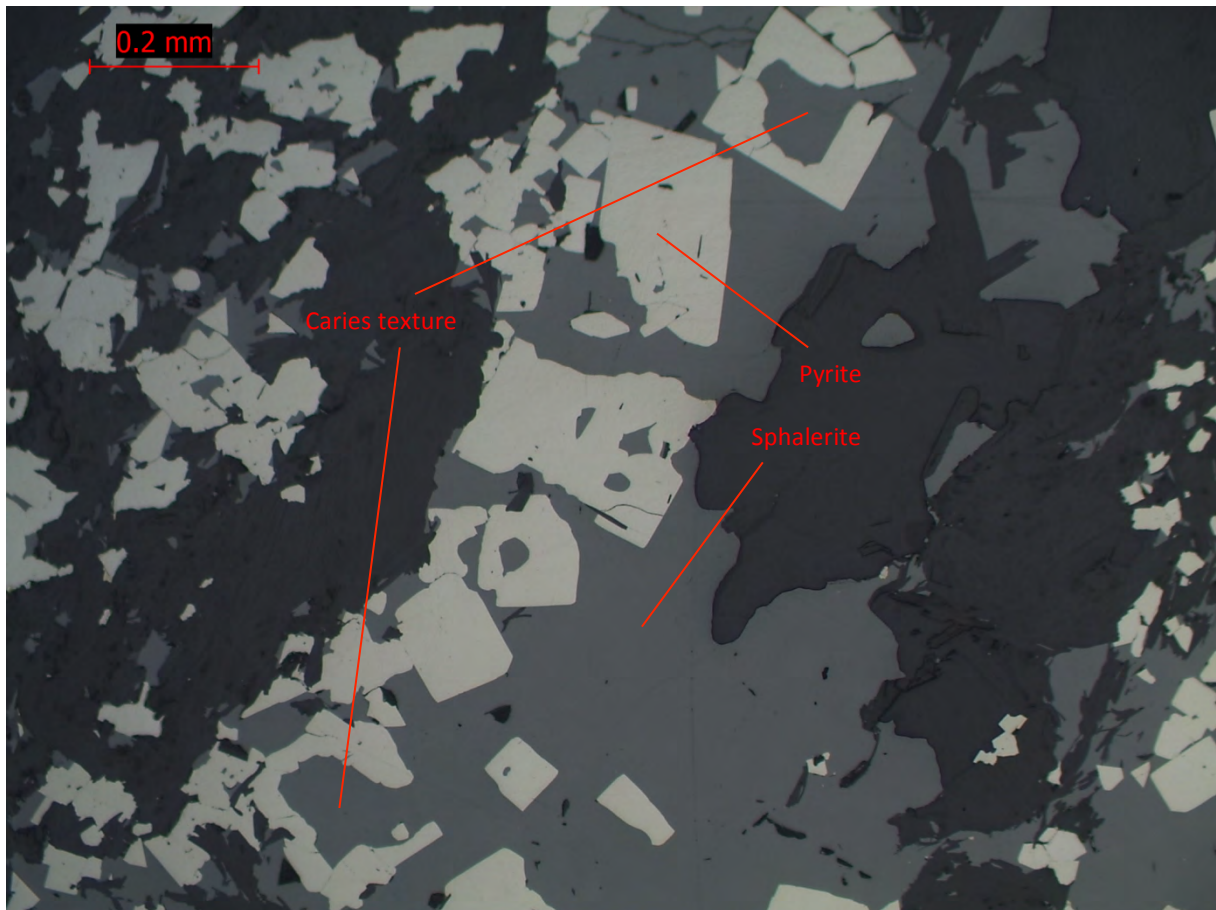


Fig.8. Pyrite cubes with caries texture where the cubes are being replaced by sphalerite from the inside out.

Lithology: Sphalerite-rich massive sulfide

Opaque minerals: Pyrite (20 %), chalcopyrite (5 %), arsenopyrite (<5 %), pyrrhotite (<1 %), sphalerite (30 %), galena (5 %) and tetrahedrite (<1 %).

Alteration minerals: Quartz, chlorite and muscovite and carbonate.

Opaque mineralogy: Mostly pyrite and sphalerite but also some chalcopyrite, pyrrhotite, galena, arsenopyrite and tetrahedrite. There are two distinct areas in the sample. One area has mostly sphalerite, galena and a few cubes of pyrite while the other area is rich in pyrite, chalcopyrite, arsenopyrite and pyrrhotite. The pyrite occurs as euhedral cubes and triangles as well as anhedral aggregates. Pyrite shows caries texture in places being replaced internally by sphalerite (Fig.8). The pyrrhotite occurs mostly as needle-shaped inclusions in sphalerite but also as occur as large subhedral to anhedral aggregates associated with sphalerite and chalcopyrite. Chalcopyrite occurs as subhedral to anhedral aggregates associated with pyrite and sphalerite. Galena occurs as subhedral to anhedral aggregates. Sphalerite is concentrated mostly on one side of the sample and occurs as subhedral to anhedral aggregates. Tetrahedrite occurs as euhedral to anhedral inclusions in galena. Arsenopyrite occurs as euhedral rhomb shapes and cubes.

Alteration mineralogy: Quartz and chlorite forms a matrix that makes up most of the sample

while the muscovite and carbonate is scattered throughout the sample as both single grains and aggregates.

RS038

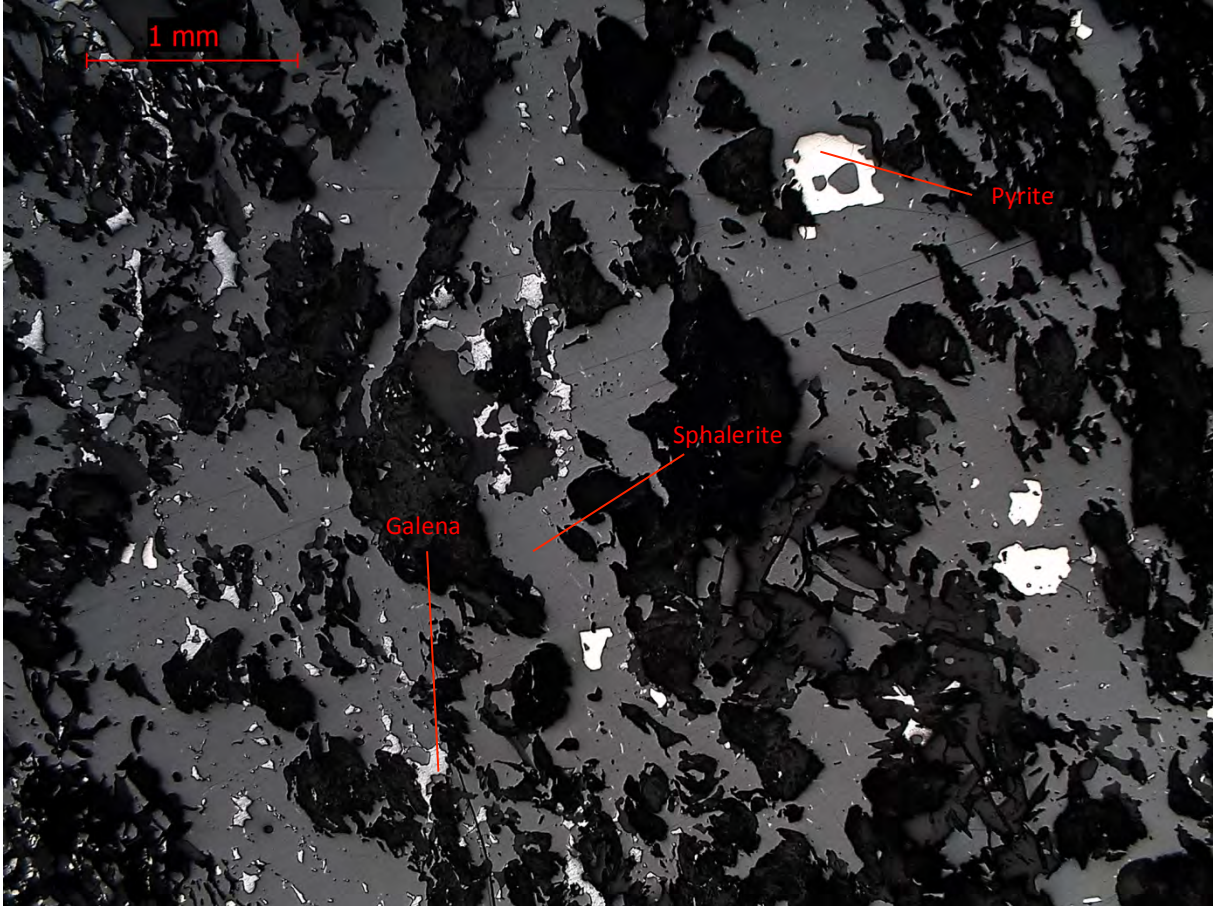


Fig.9. Small patches of pyrite and galena in a network of sphalerite.

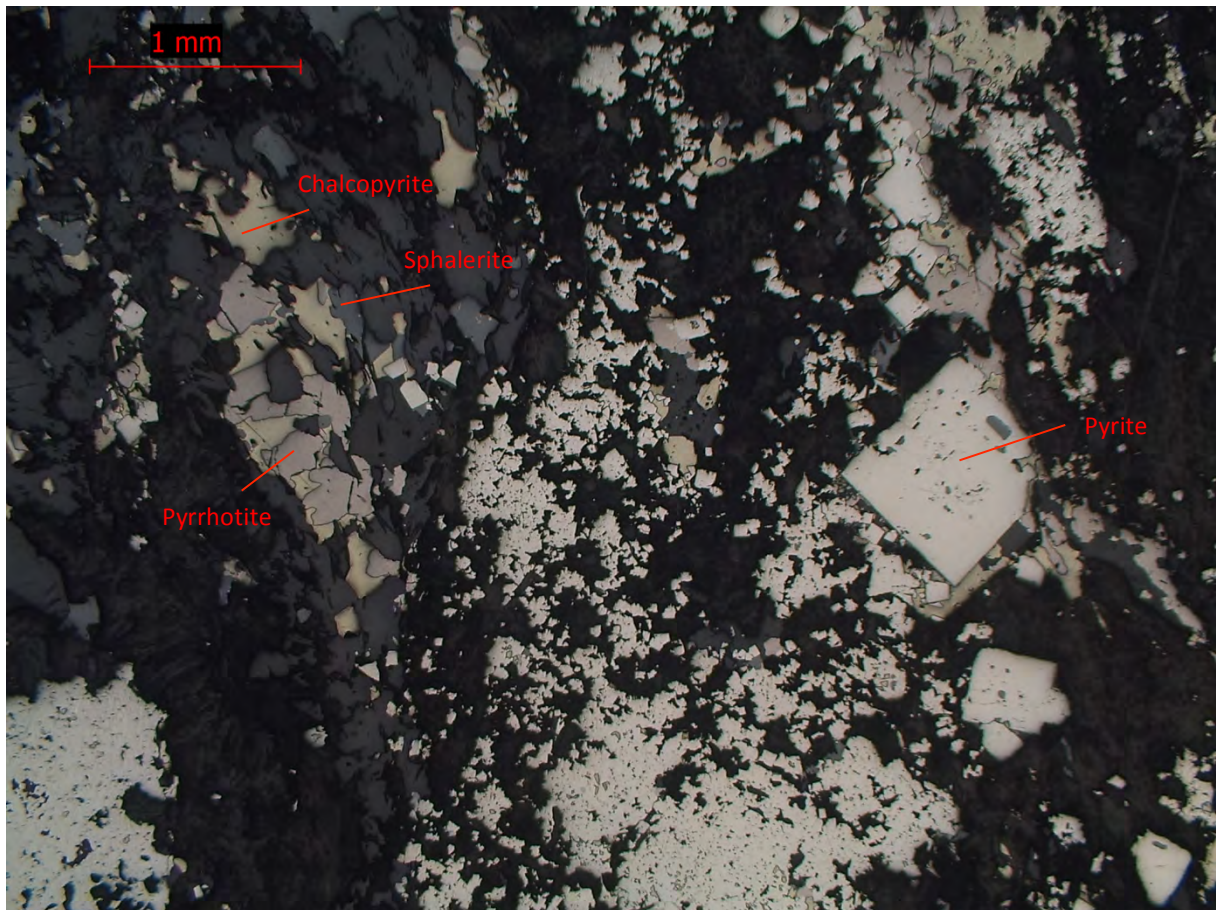


Fig.10. Patches of pyrite, chalcopyrite, pyrrhotite and sphalerite in a matrix of muscovite, chlorite and carbonate. There is also a big pyrite cube with inclusions of sphalerite and chalcopyrite.

Lithology: Mixed massive sulfide

Opaque minerals: Pyrite (25 %), chalcopyrite (<5 %), pyrrhotite (<5 %), sphalerite (25 %), galena (<5 %) and tetrahedrite (<1 %).

Alteration minerals: Quartz, chlorite, muscovite, sericite and carbonate.

Opaque mineralogy: Mostly pyrite and sphalerite but there is also some chalcopyrite, galena and tetrahedrite. There is a sharp contact between a pyrite-rich layer and a sphalerite-rich layer. The pyrite occurs as euhedral cubes and anhedral aggregates. Sphalerite occurs as skeletal aggregates and often has pyrite cubes as inclusions. Chalcopyrite is mostly concentrated in the pyrite-rich layer and occurs as large subhedral to anhedral aggregates and as small subhedral inclusions in pyrite and sphalerite. Galena occurs as subhedral to anhedral inclusions in sphalerite. Pyrrhotite occurs as needle-shaped inclusions in sphalerite and as subhedral to anhedral aggregates scattered throughout the sample. Tetrahedrite occurs as subhedral to anhedral inclusions in galena. Carbonate makes up the matrix that fills up the spaces between the other minerals.

Alteration mineralogy: Muscovite, chlorite and carbonate forms a matrix that makes up most of the sample while quartz occurs as scattered aggregates. There is also sericite in the matrix

associated with quartz.

RS050

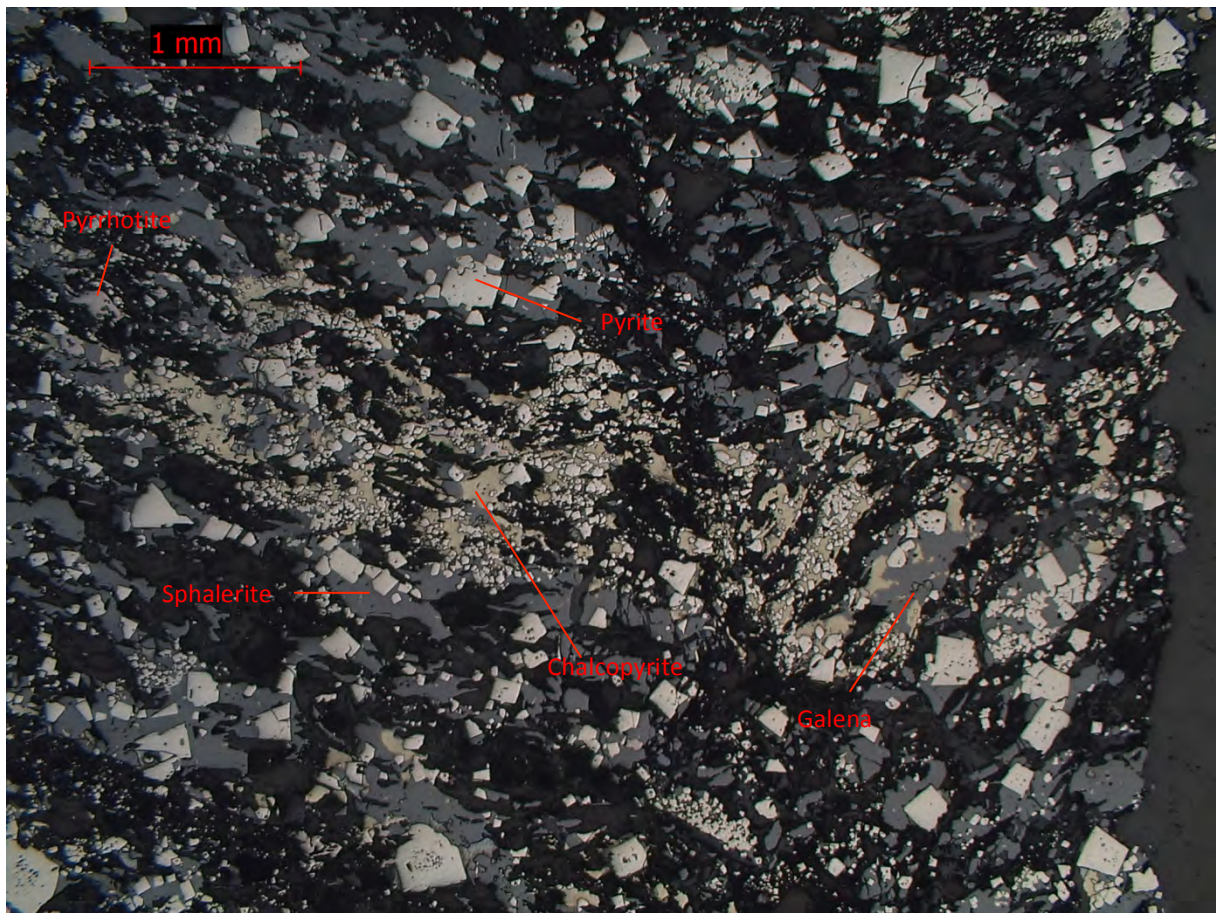


Fig.11. Layers with resorbed pyrite and sphalerite and layers with patches of chalcopyrite, galena and pyrrhotite. There's a big carbonate vein on the right side of the photo.

Lithology: Mixed massive sulfide

Opaque minerals: Pyrite (30 %), chalcopyrite (5 %), pyrrhotite (<1 %), sphalerite (30 %), galena (5 %) and tetrahedrite (<1 %).

Alteration minerals: Quartz, sericite, actinolite and carbonate.

Alteration mineralogy: Mostly pyrite and sphalerite but also some chalcopyrite, pyrrhotite, galena and tetrahedrite. The pyrite occurs as euhedral cubes and anhedral aggregates. The pyrite ranges in size from large cubes to tiny euhedral to anhedral grains. Pyrite shows caries texture in places being replaced internally by sphalerite. Chalcopyrite occurs as subhedral to anhedral inclusions and as larger aggregates associated with pyrite. Sphalerite occurs as subhedral to anhedral, skeletal aggregates. Galena occurs as inclusions in sphalerite. Pyrrhotite occurs as needle-shaped inclusion in sphalerite. Tetrahedrite occurs as subhedral to anhedral inclusions in galena. The sample is layered with layers rich with partially resorbed pyrite and layers rich with the other sulfides.

Opaque mineralogy: Mostly actinolite and carbonate forming a network in the space between the alteration minerals. There is some quartz occurring as aggregates and sericite associated with the quartz. There is a big carbonate vein in the middle of the sample.

RS053

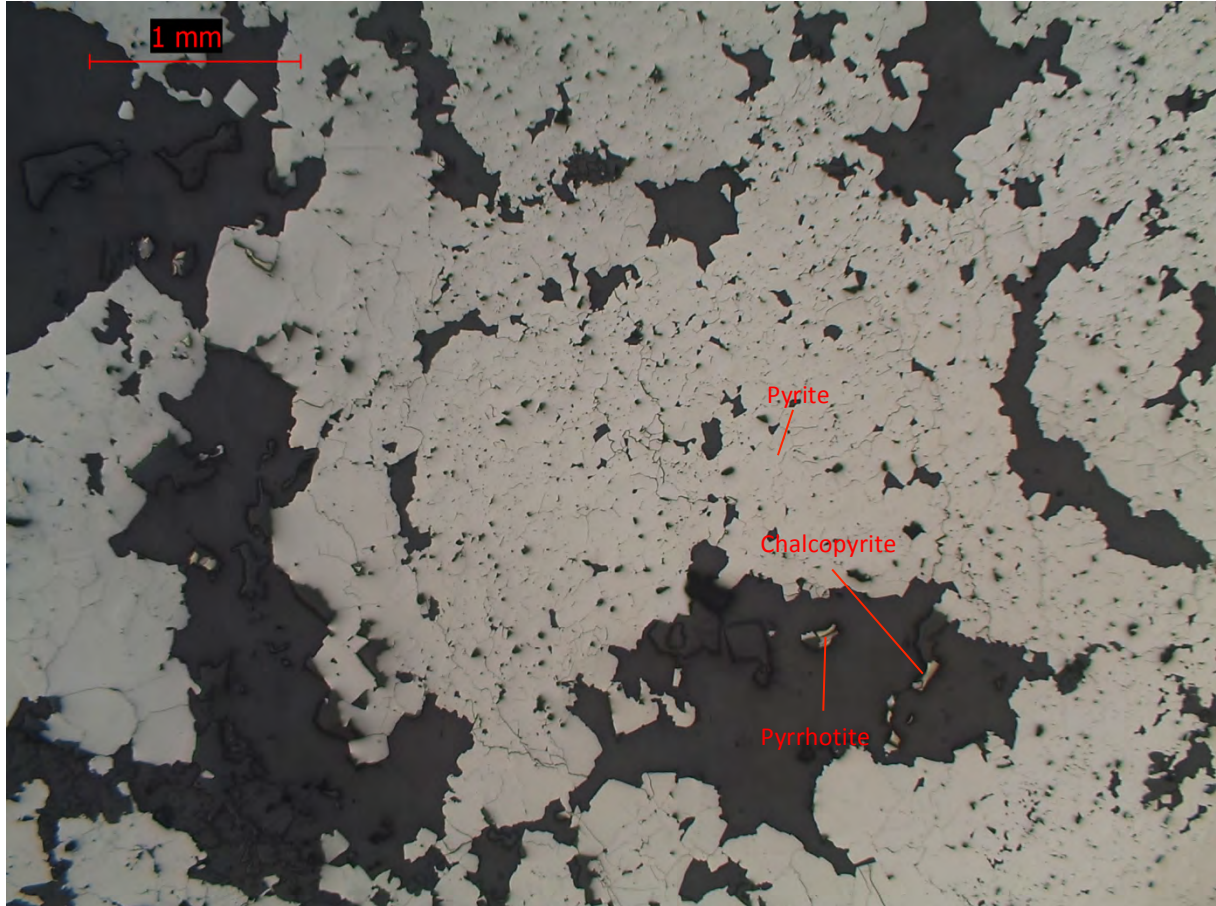


Fig.12. Intergranular pyrite and small grains of chalcopyrite and pyrrhotite in patches of carbonate.

Lithology: Pyrite-rich massive sulfide

Opaque minerals: Pyrite (80 %), chalcopyrite (<1 %) and pyrrhotite (<1 %).

Alteration minerals: Quartz, actinolite and carbonate.

Opaque mineralogy: Pyrite is by far the most abundant mineral but there is also some chalcopyrite and carbonate. The pyrite mostly occurs as anhedral aggregates forming an intergranular texture but there are also some euhedral grains as well. The chalcopyrite occurs as subhedral grains inside the pyrite aggregates.

Alteration mineralogy: Mostly a matrix of quartz and carbonate forming a network of "islands". There are also some aggregates of actinolite.

RS058

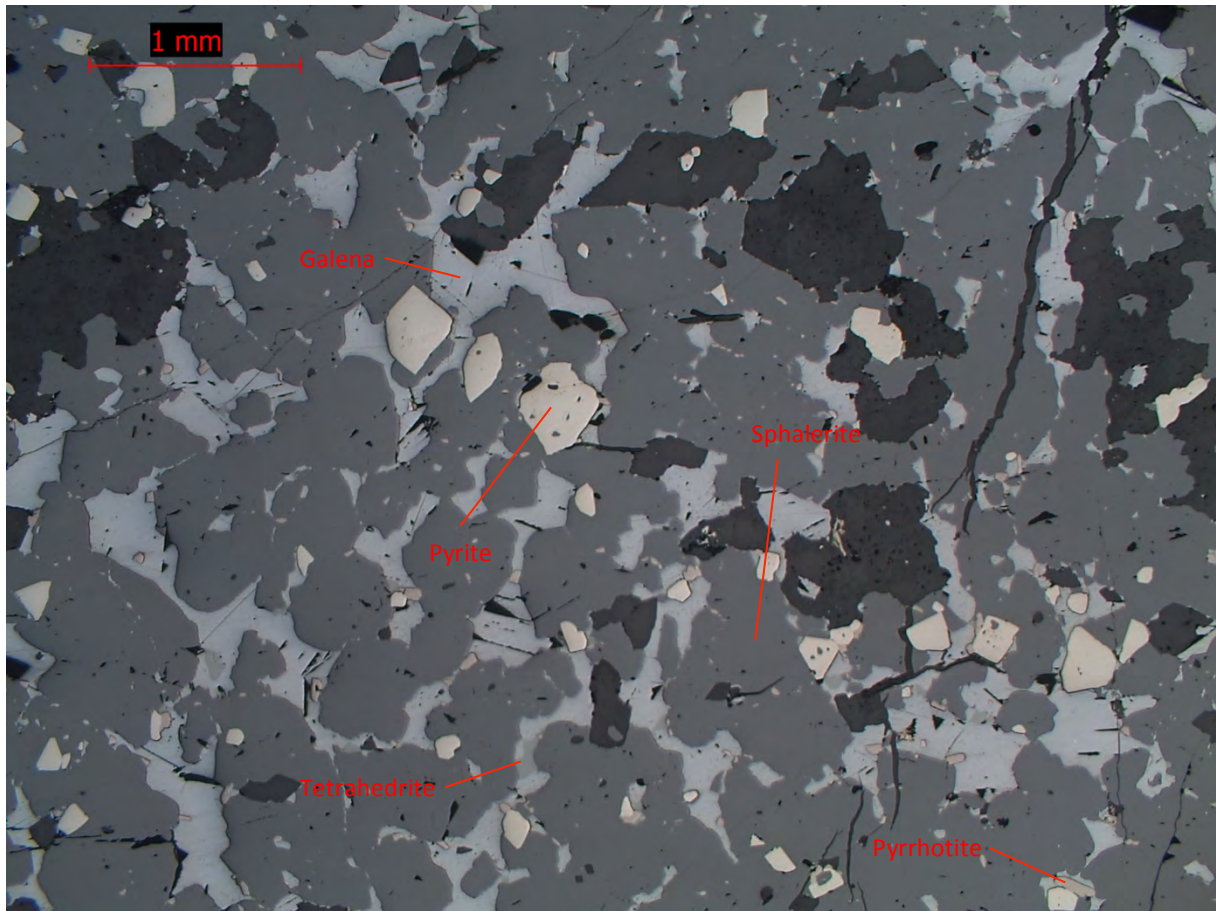


Fig.13. Patches of pyrite, galena and pyrrhotite in a matrix of sphalerite. Small patches of tetrahedrite in galena.

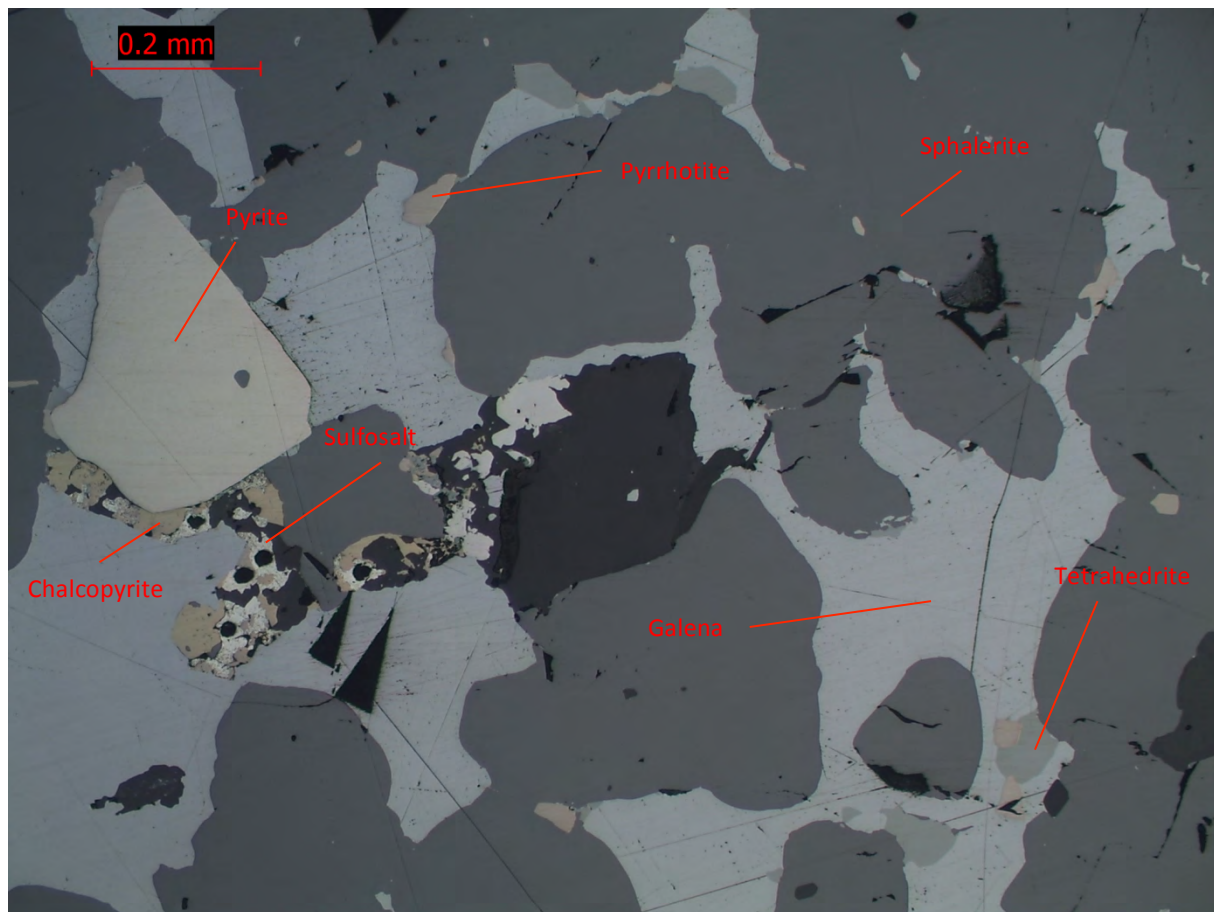


Fig.14. Closer look at tetrahedrite showing that they are relatively abundant in this sample. The black triangles in are triangular pits that are common in galena and the black round holes are laser ablation pits.

Lithology: Sphalerite-rich massive sulfide

Opaque minerals: Pyrite (<10 %), chalcopyrite (<1 %), pyrrhotite (<1 %), sphalerite (70 %), galena (<10 %) and tetrahedrite (<1 %).

Alteration minerals: Quartz, muscovite and carbonate.

Opaque mineralogy: Mostly sphalerite and carbonate with sphalerite being the most dominant. There is also some pyrite, chalcopyrite, pyrrhotite, galena and tetrahedrite. The sphalerite occurs as an anhedral mass with the carbonate and galena filling up the spaces in between. The pyrite occurs as cubes scattered throughout the sample. Chalcopyrite occurs as small anhedral grains associated with carbonate. Pyrrhotite occurs as subhedral to anhedral inclusions in sphalerite. Tetrahedrite is relatively abundant compared to the other amples and occurs as inclusions in galena as seen in (Fig. x). There are several carbonate veins in the sample. Tetrahedrite has been altered to sulfosalts in some places, usually areas where chalcopyrite, pyrrhotite and carbonate surrounds tetrahedrite.

Alteration mineralogy: Mostly carbonate and muscovite occurring as scattered “islands” that are sometimes linked by veins. There are several carbonate veins in the sample and some scattered quartz grains.

RS060

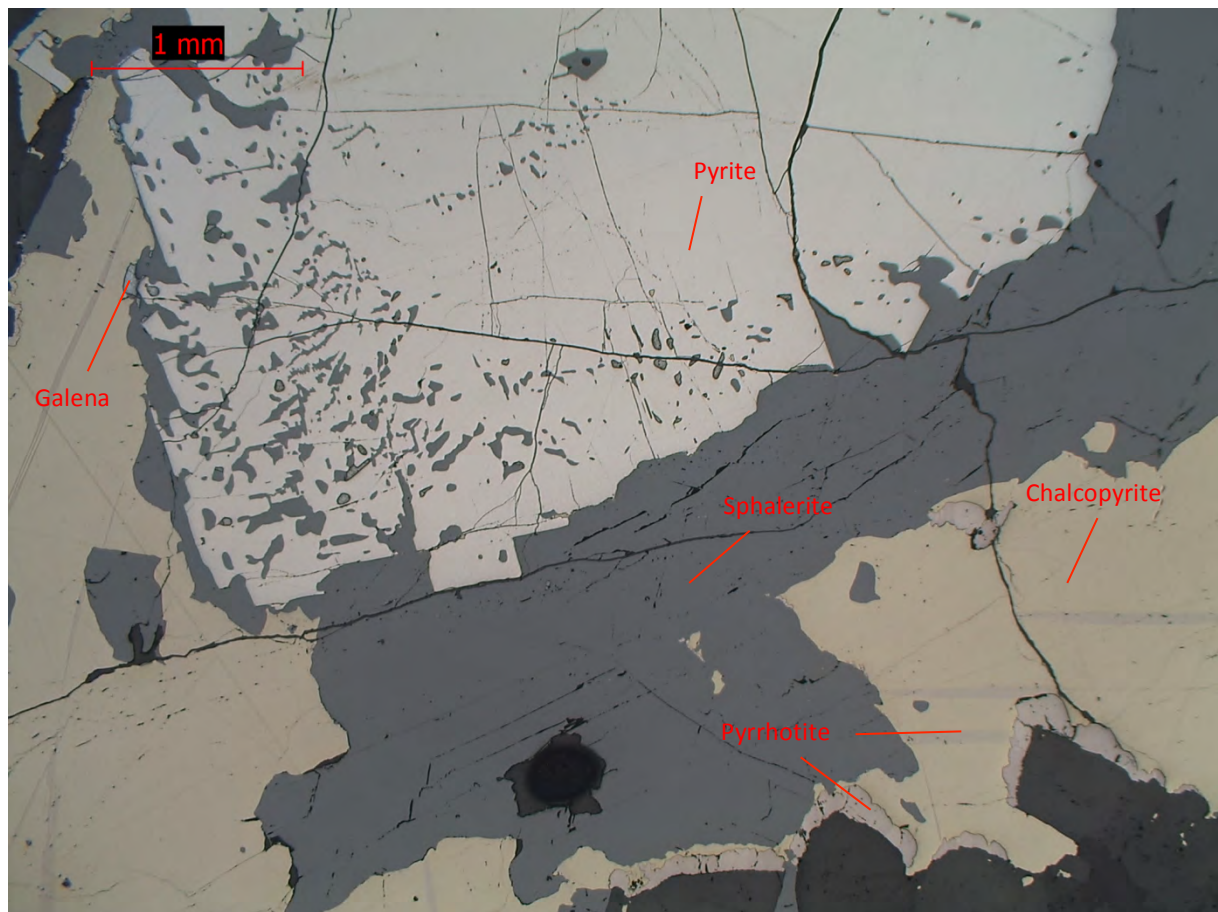


Fig.15. Big patches of pyrite, sphalerite and chalcopyrite. Pyrrhotite occurs along the rim and as streaks in chalcopyrite. Galena occurs as inclusions in sphalerite. Pyrite shows a replacement texture where pyrite is being replaced by sphalerite.

Lithology: Mixed massive sulfide

Opaque minerals: Pyrite (5 %), chalcopyrite (5 %), pyrrhotite (<1 %), sphalerite (5 %) and galena (<1 %).

Alteration minerals: Carbonate.

Opaque mineralogy: One big inclusion/vein and a smaller vein both of which consists of pyrite, chalcopyrite, pyrrhotite, sphalerite and galena. The pyrite, chalcopyrite, sphalerite in the big inclusion/vein have large grain sizes and are euhedral to subhedral. In the smaller vein the grain sizes are smaller and are mostly subhedral to anhedral. Pyrrhotite occurs as subhedral to anhedral aggregates along the edge of the big inclusion/vein.

Alteration mineralogy: Carbonate makes up more than 80% of the sample and forms a fine grained matrix. The sulfides occur where the carbonate is more coarse-grained.

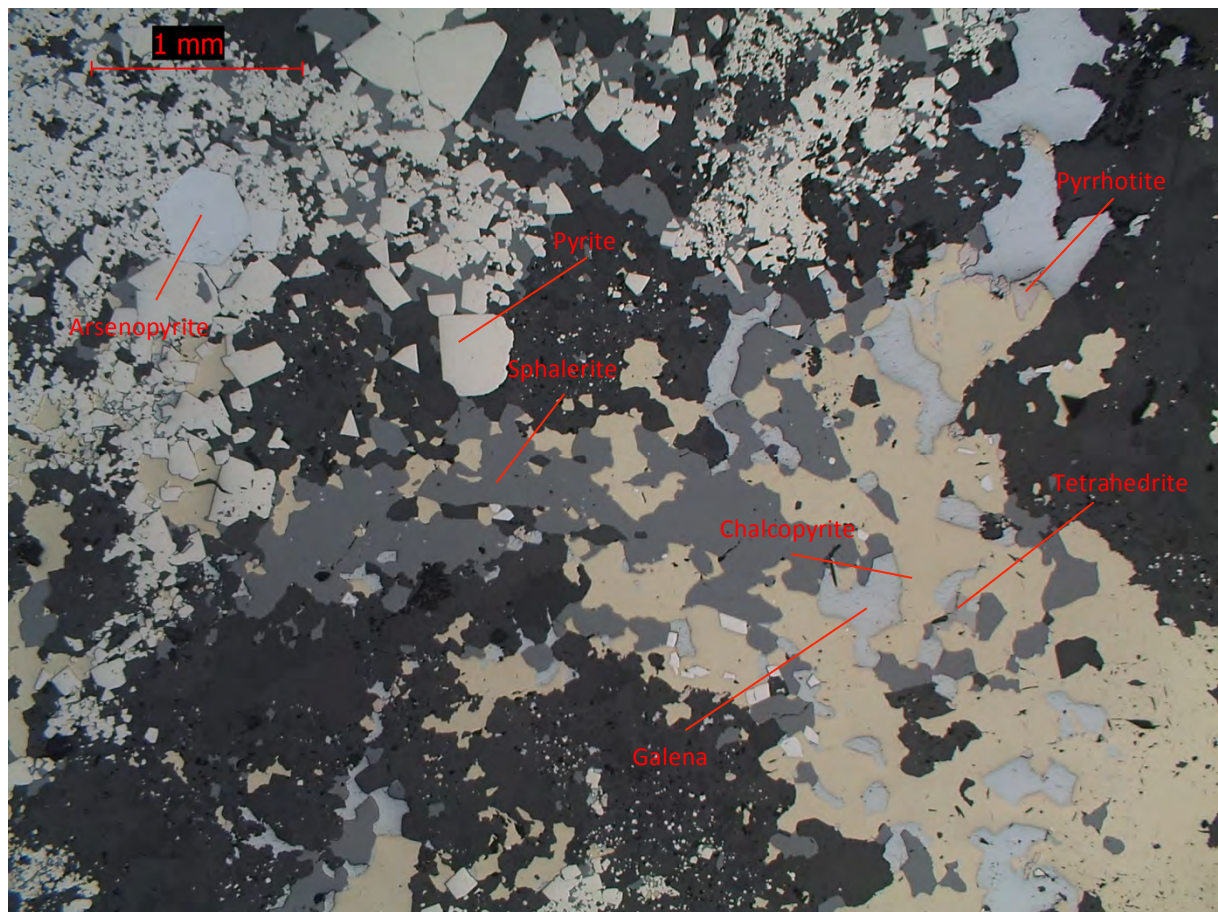


Fig.16. Large patches of pyrite, chalcopyrite, sphalerite, galena and pyrrhotite. There is also some arsenopyrite shaped as cubes or rhombs as well as a few small patches of tetrahedrite in galena.

Lithology: Mixed massive sulfide

Opaque minerals: Pyrite (30 %), chalcopyrite (10 %), pyrrhotite (<1 %), arsenopyrite (<1 %), sphalerite (15 %), galena (5 %) and tetrahedrite (<1 %).

Alteration minerals: Quartz, actinolite and carbonate.

Opaque mineralogy: Pyrite, chalcopyrite, sphalerite and carbonate are all very abundant. There is also some galena, pyrrhotite, arsenopyrite and tetrahedrite. The pyrite occurs as euhedral cubes and as anhedral aggregates. Arsenopyrite occurs as euhedral cubes. Chalcopyrite, sphalerite, galena and pyrrhotite occur as subhedral to anhedral aggregates. Tetrahedrite occurs as inclusions in galena.

Alteration mineralogy: Mostly carbonate forming a network of “islands” as well as a big inclusion. Quartz and actinolite occurs as aggregates associated with carbonate.

RS073

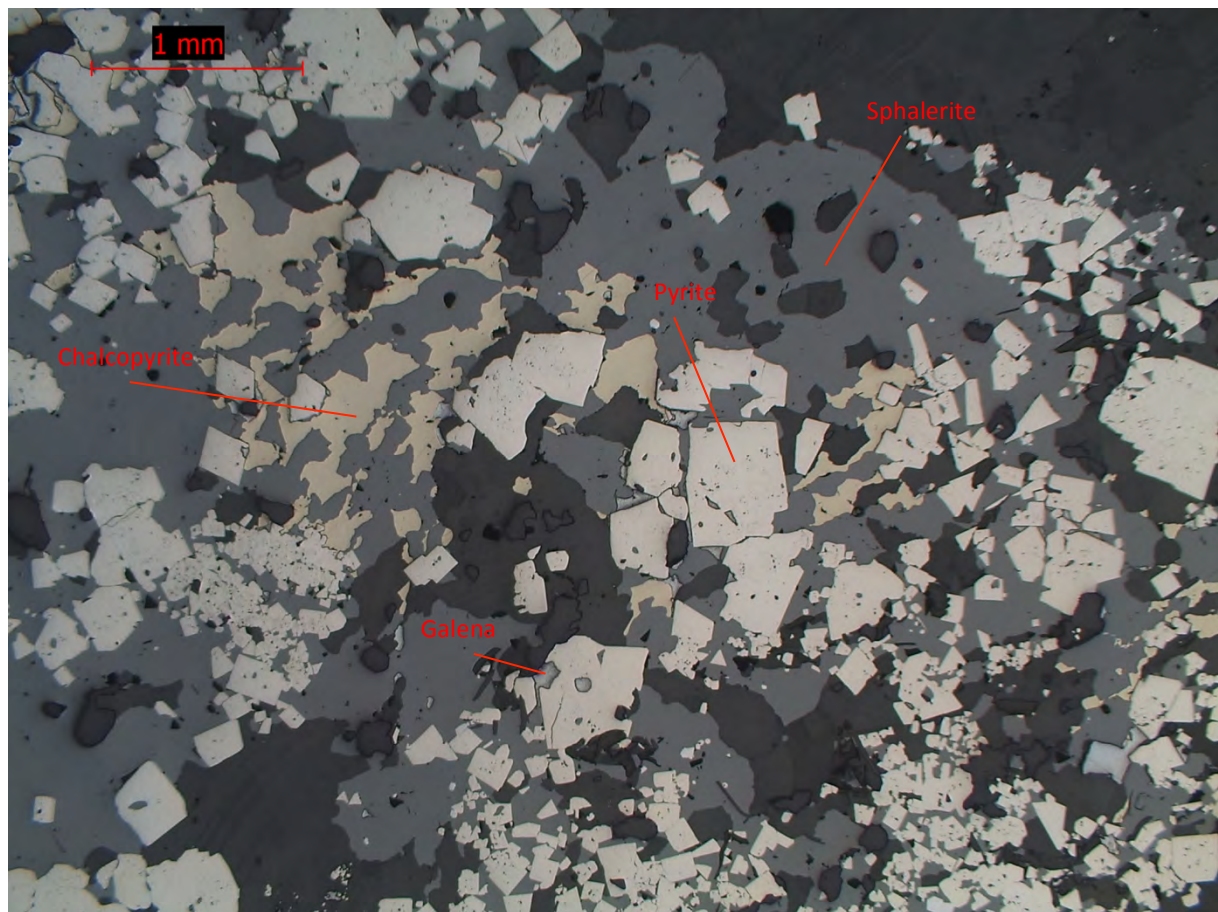


Fig.17. Cubes of pyrite in patches of sphalerite and chalcopyrite. Galena occurs as inclusions in pyrite and small patches in sphalerite.

Lithology: Pyrite-rich massive sulfide

Opaque minerals: Pyrite (35 %), chalcopyrite (5 %), pyrrhotite (<1 %), arsenopyrite (<5 %), sphalerite (15 %), galena (<5 %) and tetrahedrite (<1 %).

Alteration minerals: Quartz, actinolite and carbonate.

Opaque mineralogy: Mostly pyrite but chalcopyrite, sphalerite, galena and arsenopyrite are also relatively abundant and occur around the pyrite. There is also some pyrrhotite and tetrahedrite. The pyrite is mostly euhedral and forms a network of cubes. Chalcopyrite, sphalerite and galena occur in the spaces between the cubes and are subhedral to anhedral occurring as both aggregates and individual grains. Arsenopyrite occurs as scattered euhedral cubes and subhedral grains. Pyrrhotite occurs as small subhedral to anhedral grains. Tetrahedrite occurs as inclusions in galena.

Alteration mineralogy: Mostly carbonate forming a network of “islands” as well as a big inclusion. There are also some scattered aggregates and single grains of quartz and actinolite.

RS077

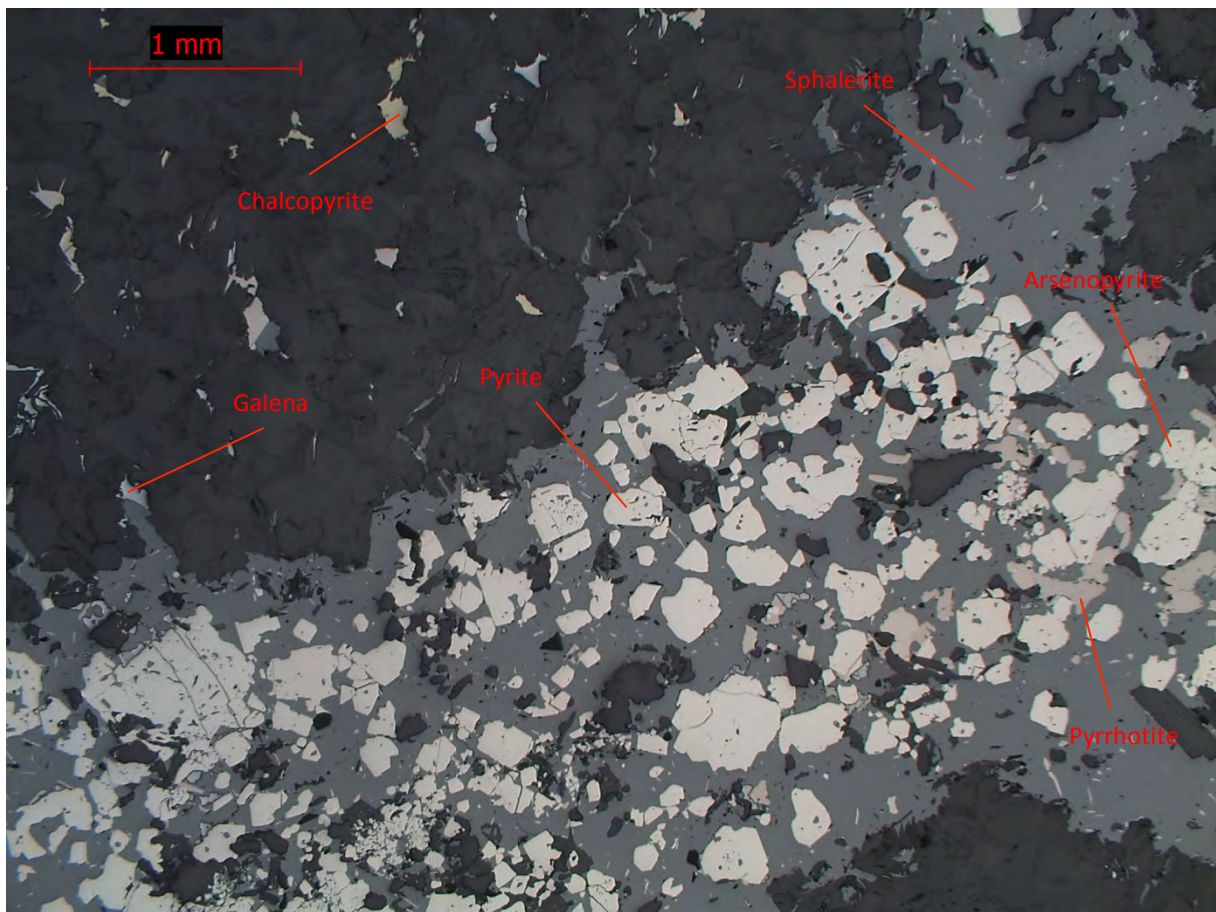


Fig.18. A network of sphalerite with cubes of arsenopyrite and patches of pyrite and pyrrhotite in a carbonate matrix. Some small patches of chalcopyrite and galena associated with carbonate.



Fig.19 Chlorite with fan texture.

Lithology: Sphalerite-rich massive sulfide

Opaque minerals: Pyrite (20 %), chalcopyrite (<1 %), pyrrhotite (<1 %), arsenopyrite (<5 %), sphalerite (15 %), galena (1 %) and tetrahedrite (<1 %).

Alteration minerals: Muscovite, chlorite and carbonate.

Opaque mineralogy: A groundmass of quartz with big clusters of pyrite, chalcopyrite, sphalerite, galena and arsenopyrite. The pyrite occurs as euhedral cubes and anhedral aggregates. Sphalerite occurs as subhedral to anhedral aggregates. Galena occurs as small anhedral aggregate associated with sphalerite. Chalcopyrite occurs as small anhedral aggregates. Arsenopyrite occurs as euhedral cubes scattered throughout the sample. Pyrrhotite occurs as needle-shaped inclusion in galena. Tetrahedrite occurs as inclusions in galena.

Alteration mineralogy: Mostly a matrix of chlorite forming a network of “islands”. The chlorite in this sample are relatively undeformed and show fan texture as seen in (Fig. x). Muscovite occurs as scattered grains. Carbonate occurs as large subhedral grains in a vein along one of the edges of the sample.

RS081



Fig.20. Grains of pyrite and pyrrhotite in different sizes in a matrix of quartz, carbonate, chlorite and biotite. A big clast surrounds the big pyrite grain.

Lithology: Volcanogenic sediment

Opaque minerals: Pyrite (<5 %), chalcopyrite (<1 %), pyrrhotite (<1 %), arsenopyrite (<1 %) and ilmenite/titanite (<1 %).

Alteration minerals: Quartz, chlorite, biotite and carbonate.

Opaque mineralogy: Some scattered subhedral to anhedral grains of pyrite, chalcopyrite and arsenopyrite. Skeletal ilmenite has been strongly replaced by titanite. The ilmenite/titanite is scattered throughout the sample as individual grains.

Alteration mineralogy: Quartz and carbonate are vary abundant and appears both as a part of the matrix, as aggregates and as large clasts. Chlorite and biotite occur as part of the matrix.



Fig.21. Small grains of pyrite and pyrrhotite in a matrix of quartz, carbonate and actinolite. Several large clasts of quartz and carbonate occur in the matrix. The marked pyrite and pyrrhotite are in the pressure shadow between two clasts because of deformation.

Lithology: Pumice bearing volcanogenic sediment

Opaque minerals: Pyrite (<5 %), chalcopyrite (<1 %), arsenopyrite (<1 %), pyrrhotite (<5 %) and ilmenite/titanite (<1 %).

Alteration minerals: Quartz, biotite, actinolite and carbonate.

Opaque mineralogy: Some scattered euhedral to anhedral grains of pyrite, chalcopyrite, pyrrhotite and arsenopyrite. Skeletal ilmenite has been strongly replaced by titanite. Some of the pyrite is disseminated. The ilmenite/titanite is scattered throughout the sample as individual grains. There are a few grains of pyrrhotite in pressure shadow as seen in (Fig. x).

Alteration mineralogy: Quartz and carbonate is very abundant and occurs in both the matrix and as large clasts. Actinolite which is also abundant and appears in the matrix creates a fine-grained foliation around coarser grains. Biotite occurs as scattered grains.

SEM data

RS058

Six areas in RS058 where tetrahedrite and sulfosalts are present were chosen and then analyzed in order to identify them. The surrounding minerals were also analyzed and the results are present in the tables below. The analyses are not quantitative and the O in the samples is because of poorly polished thin-sections. There are several Ag-Sb sulfosalts in the examined areas and it's unclear exactly what they are but in (Fig.22) is a list of possible minerals they could be.

Mineral	Ag (wt %)	Sb (wt %)
Cupropolybasite	48.25	12.10
Dyscrasite	72.66	27.34
Freibergite	40.25	18.93
Pyrrargyrite	59.75	22.48
Pyrostilpnite	59.75	22.48
Samsonite	46.78	26.40
Selenostephanite	57.99	13.09
Stephanite	68.33	15.42

Fig.22. Table showing minerals with Ag and Sb content in wt % that corresponds to the Ag-Sb sulfosalts found in RS058 and RS073. The data comes from the webmineral website.

Area 1

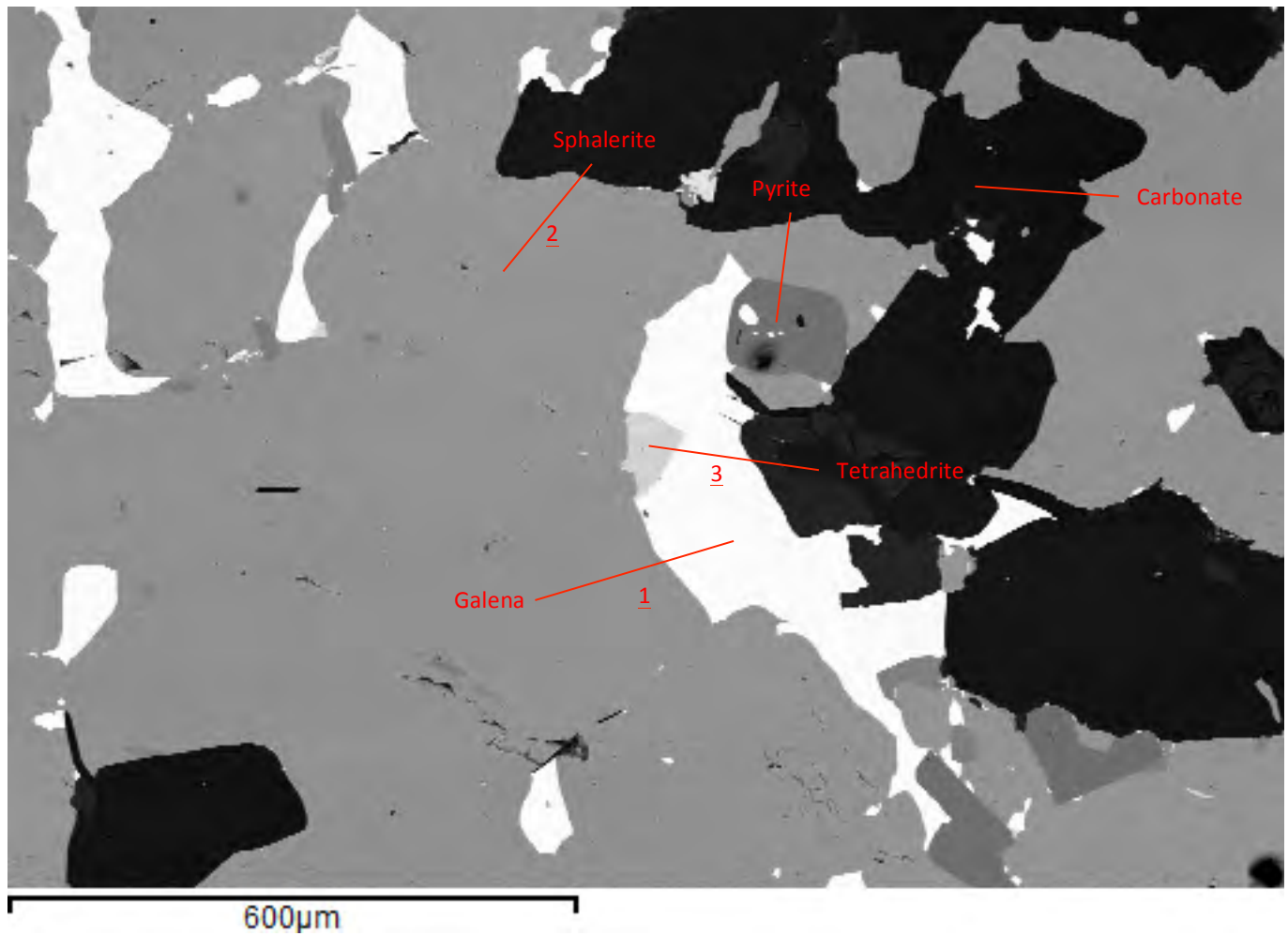


Fig.23. Photo showing area 1.

Spectrum	S (atomic %)	O	Fe	Cu	Zn	Pb	Ag	Sb	Ca	As	Hg	Mineral
1	52.07					47.93						Galena
2	54.19		5.81		40.0							Sphalerite
3	46.69		5.39	19.32	0.95		13.24	14.40				Tetrahedrite

Area 2

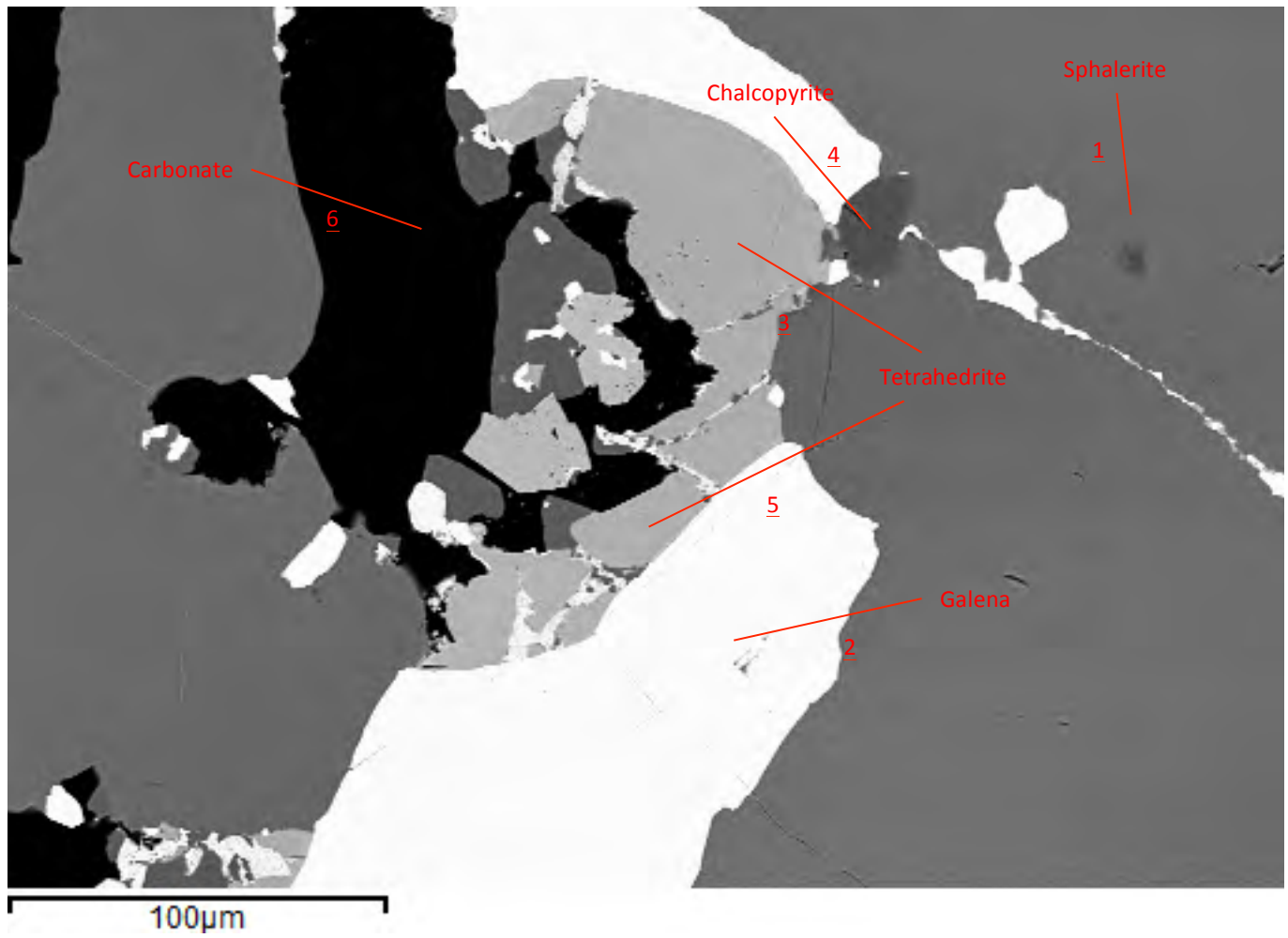


Fig.24. Photo showing area 2.

Spectrum	S (atomic %)	O	Fe	Cu	Zn	Pb	Ag	Sb	Ca	As	Hg	Mineral
1	54.08		5.81		40.11							Sphalerite
2	54.48					47.52						Galena
3	44.85	4.76	5.27	18.43	0.75		12.40	13.53				Tetrahedrite
4	54.85		22.87	22.28								Chalcopyrite
5	0.92	30.64		0.76			51.23	16.44				Tetrahedrite
6		77							23			Calcite

Area 3

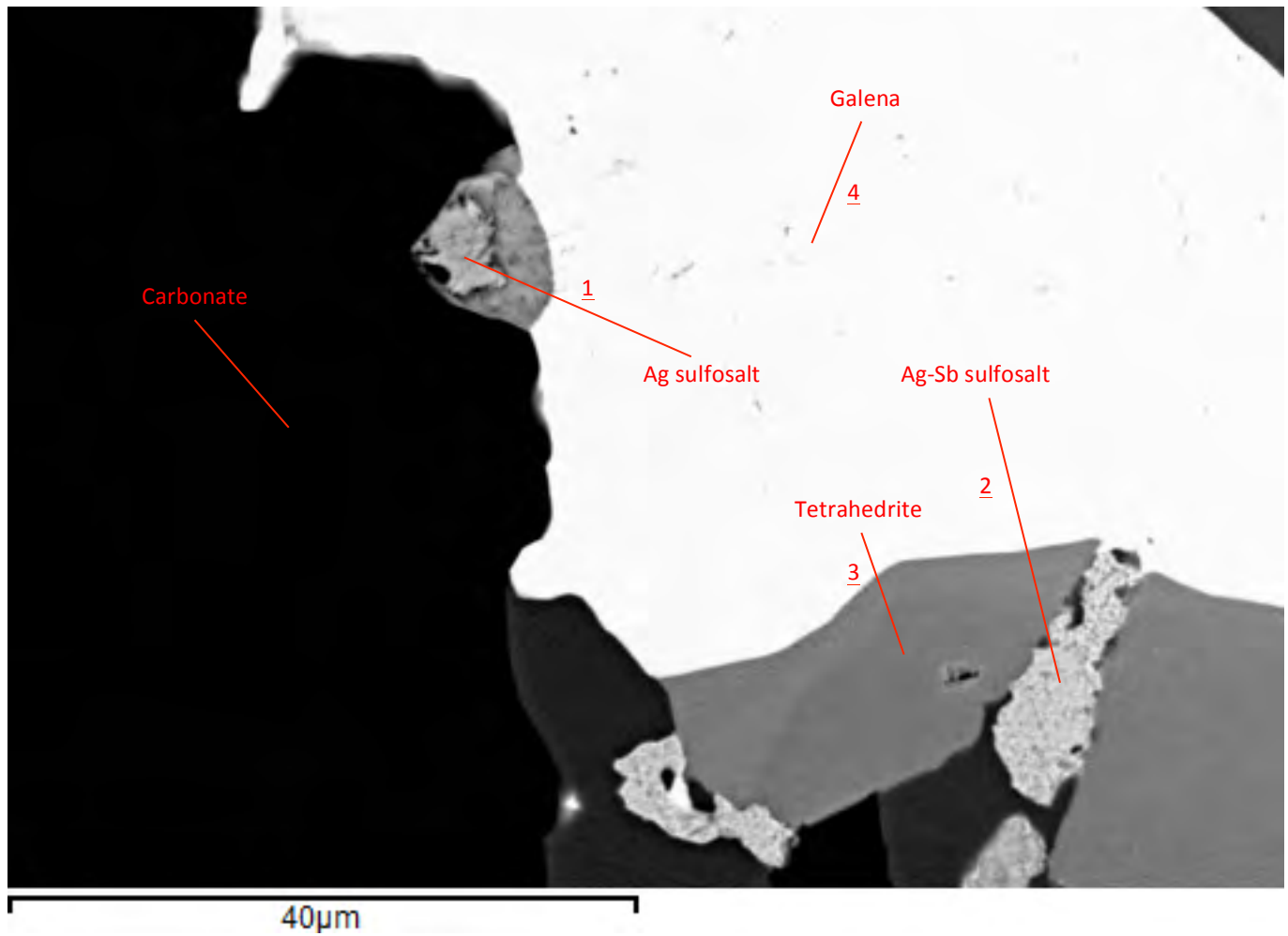


Fig.25. Photo showing area 3.

Spectrum	S (atomic %)	O	Fe	Cu	Zn	Pb	Ag	Sb	Ca	As	Hg	Mineral
1	17.13	20.46					62.41					Ag sulfosalt
2	1.21	27.18					54.31	17.30				Ag-Sb sulfosalt
3	46.83		5.58	18.88	0.86		13.42	14.44				Tetrahedrite
4	52.11					47.89						Galena

Area 4

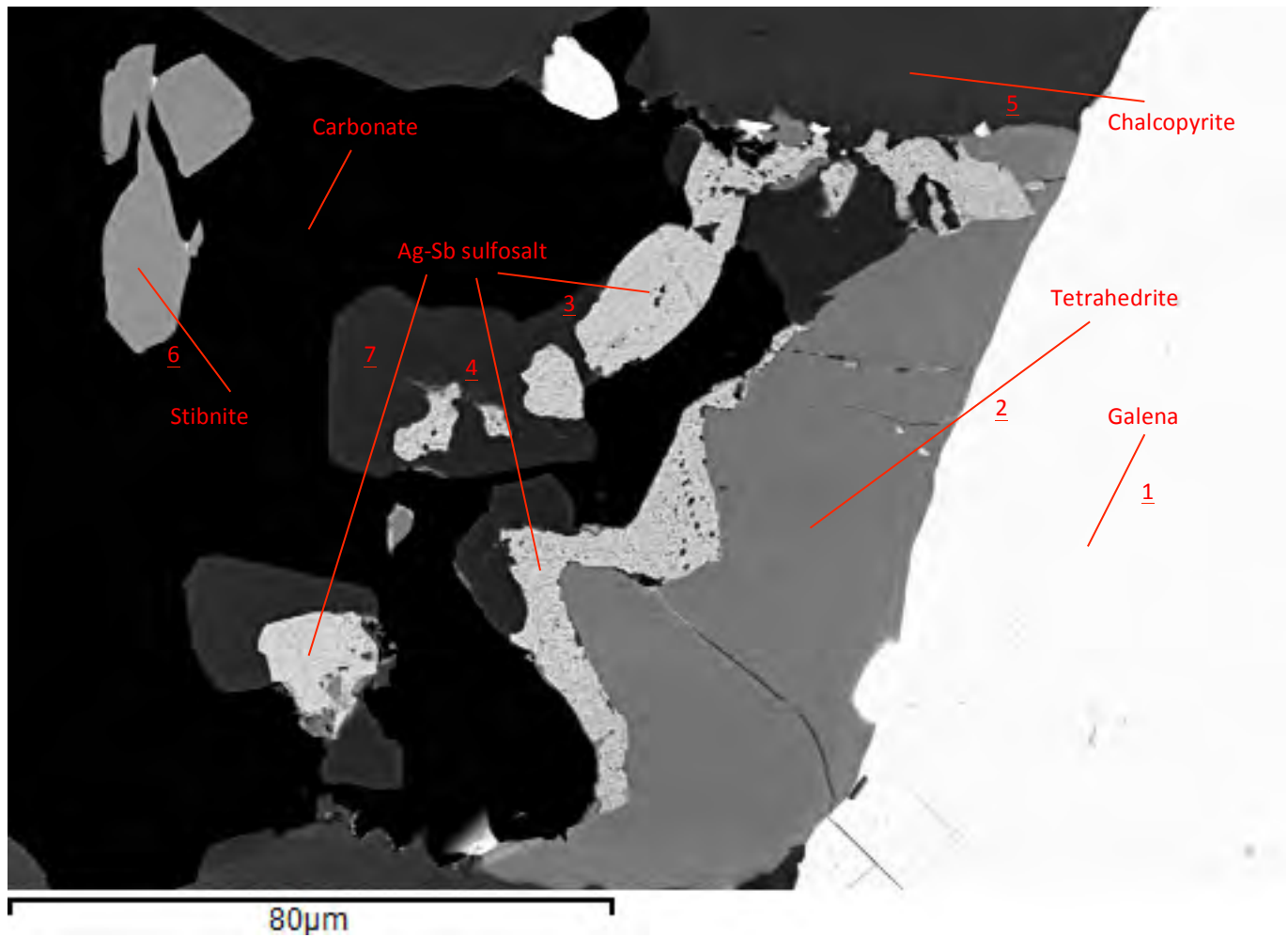


Fig.26. Photo showing area 4.

Spectrum	S (atomic %)	O	Fe	Cu	Zn	Pb	Ag	Sb	Ca	As	Hg	Mineral
1	51.33					48.69						Galena
2	46.88		5.59	19.19	1.08		12.90	14.37				Tetrahedrite
3		23.66					54.67	21.67				Ag-Sb sulfosalt
4							75.35	24.65				Ag-Sb sulfosalt
5	54.79		22.69	22.52								Chalcopyrite
6	36.36		29.97					33.67				Stibnite
7		16.24					58.65	25.10				Ag-Sb sulfosalt

Area 5

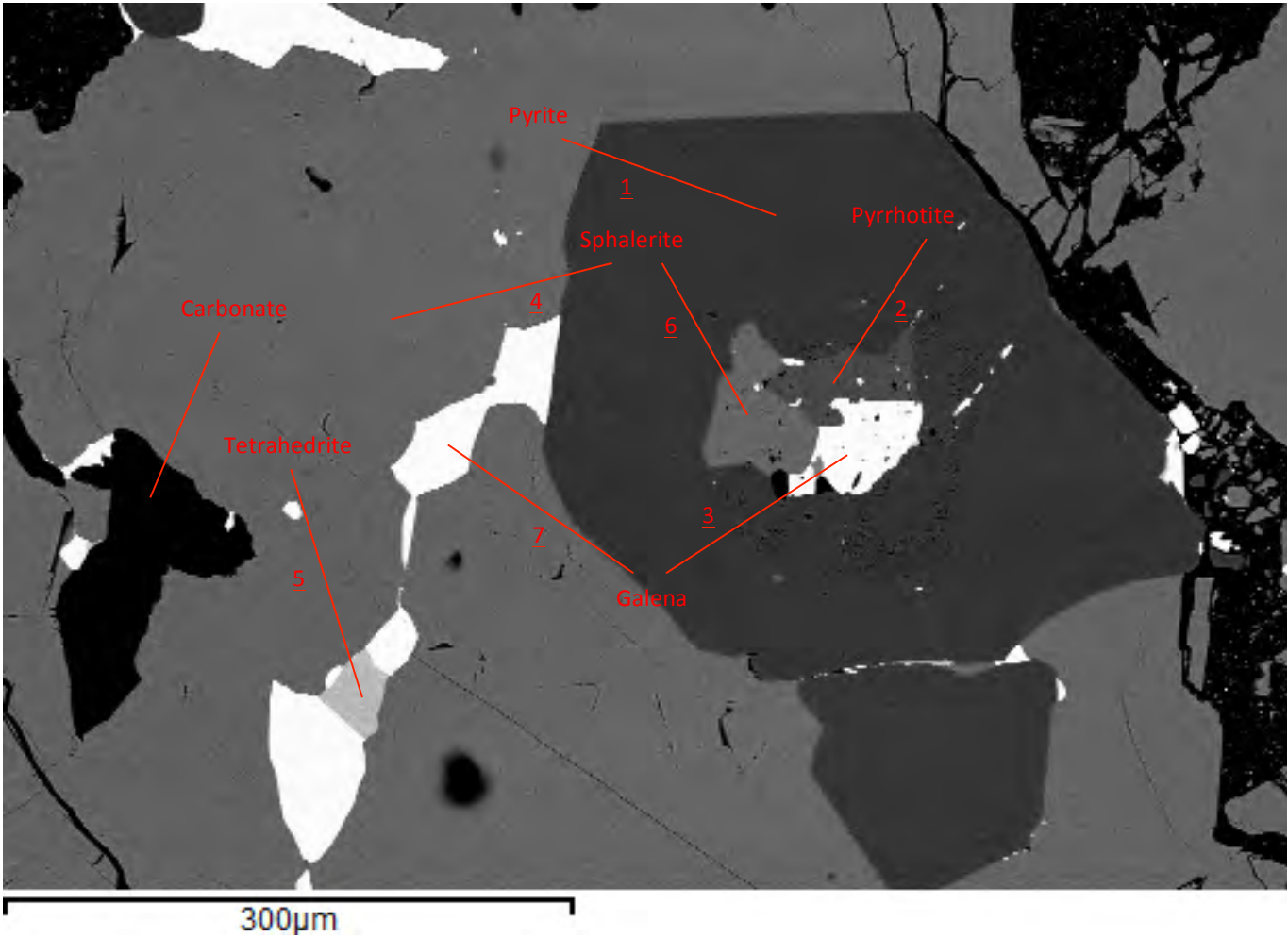


Fig.27. Photo showing area 5.

Spectrum	S (atomic %)	O	Fe	Cu	Zn	Pb	Ag	Sb	Ca	As	Hg	Mineral
1	70.15		29.85									Pyrite
2	56.95		43.05									Pyrrhotite
3	54.55		6.23			39.22						Galena
4	52.46				47.54							Sphalerite
5	44.11	5.83	5.22	17.05	1.28		13.09	13.42				Tetrahedrite
6	54.63		5.86		39.51							Sphalerite
7	51.93		1.28			46.79						Galena

Area 6

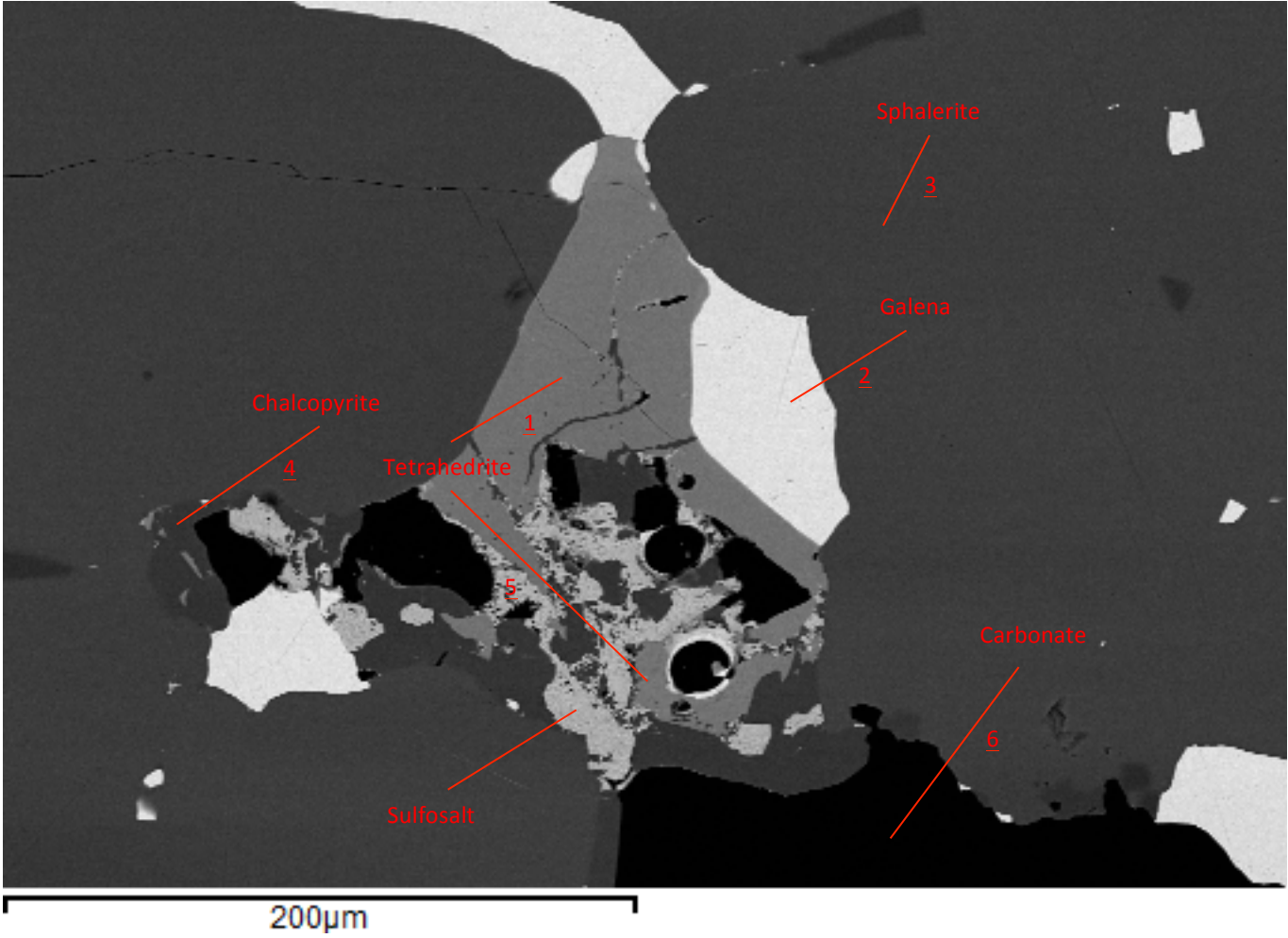


Fig.28. Photo showing area 6.

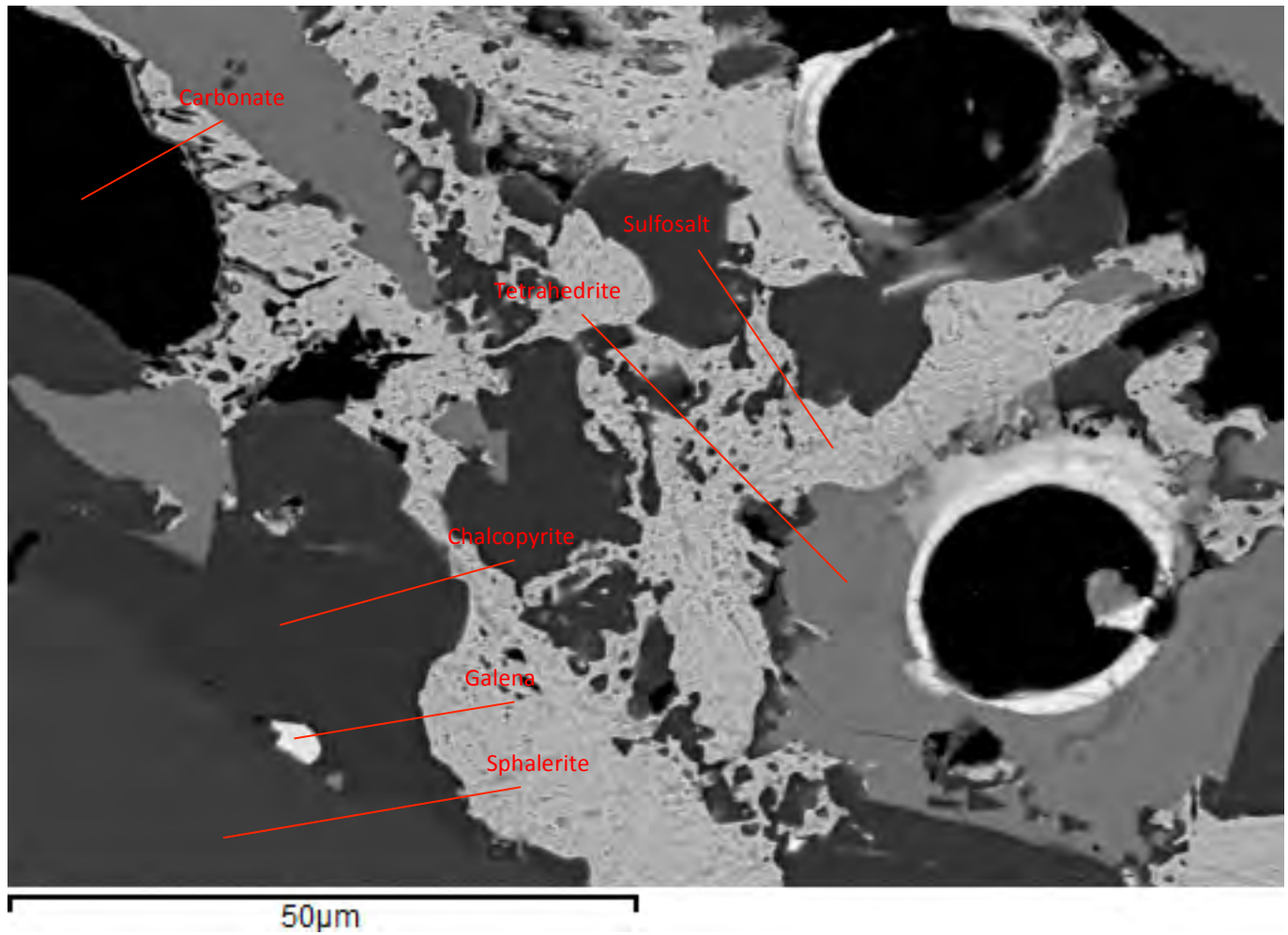


Fig.29. Photo showing a more magnified view of area 6.

Spectrum	S (atomic %)	O	Fe	Cu	Zn	Pb	Ag	Sb	Ca	As	Hg	Mineral
1	46.96		5.55	19.45	1.24		12.61	14.18				Tetrahedrite
2	52.35					47.65						Galena
3	54.86		5.85		39.29							Sphalerite
4	55.07		22.84	22.09								Chalcopyrite
5		16.02					61.72	22.26				Tetrahedrite
6		78.41							21.59			Calcite

RS073

Two areas in RS073 were chosen to analyze inclusions in pyrite and to identify sulfosalts.

Area 1

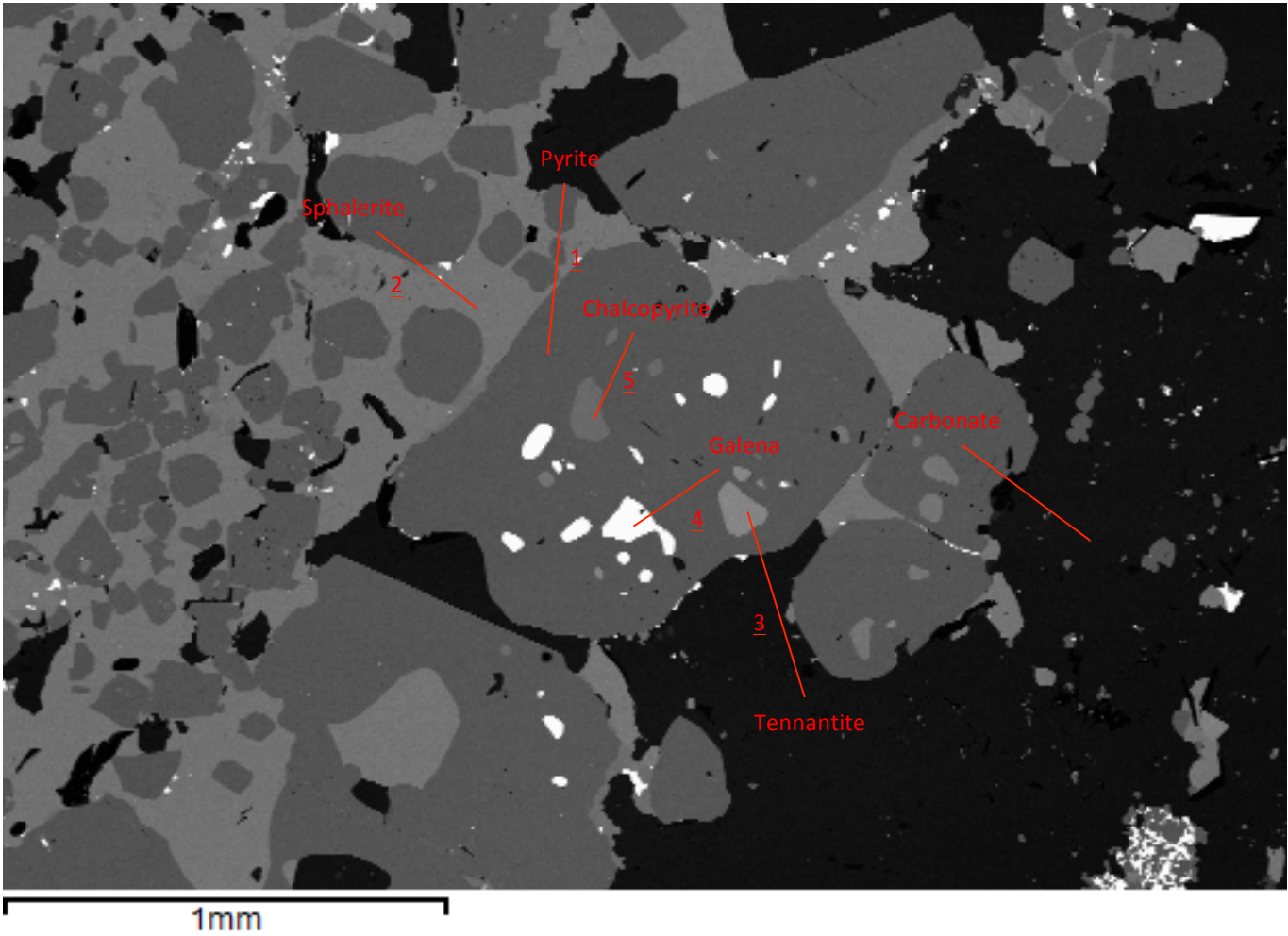


Fig.30. Photo showing area 1.

Spectrum	S (atomic %)	O	Fe	Cu	Zn	Pb	Ag	Sb	Ca	As	Hg	Mineral
1	70.22		29.78									Pyrite
2	54.22		4.05		41.73							Sphalerite
3	48.73		4.54	28.59	1.69		2.43	1.90		12.13		Tennantite
4	54.26					45.74						Galena
5	54.90		23.05	22.05								Chalcopyrite

Area 2

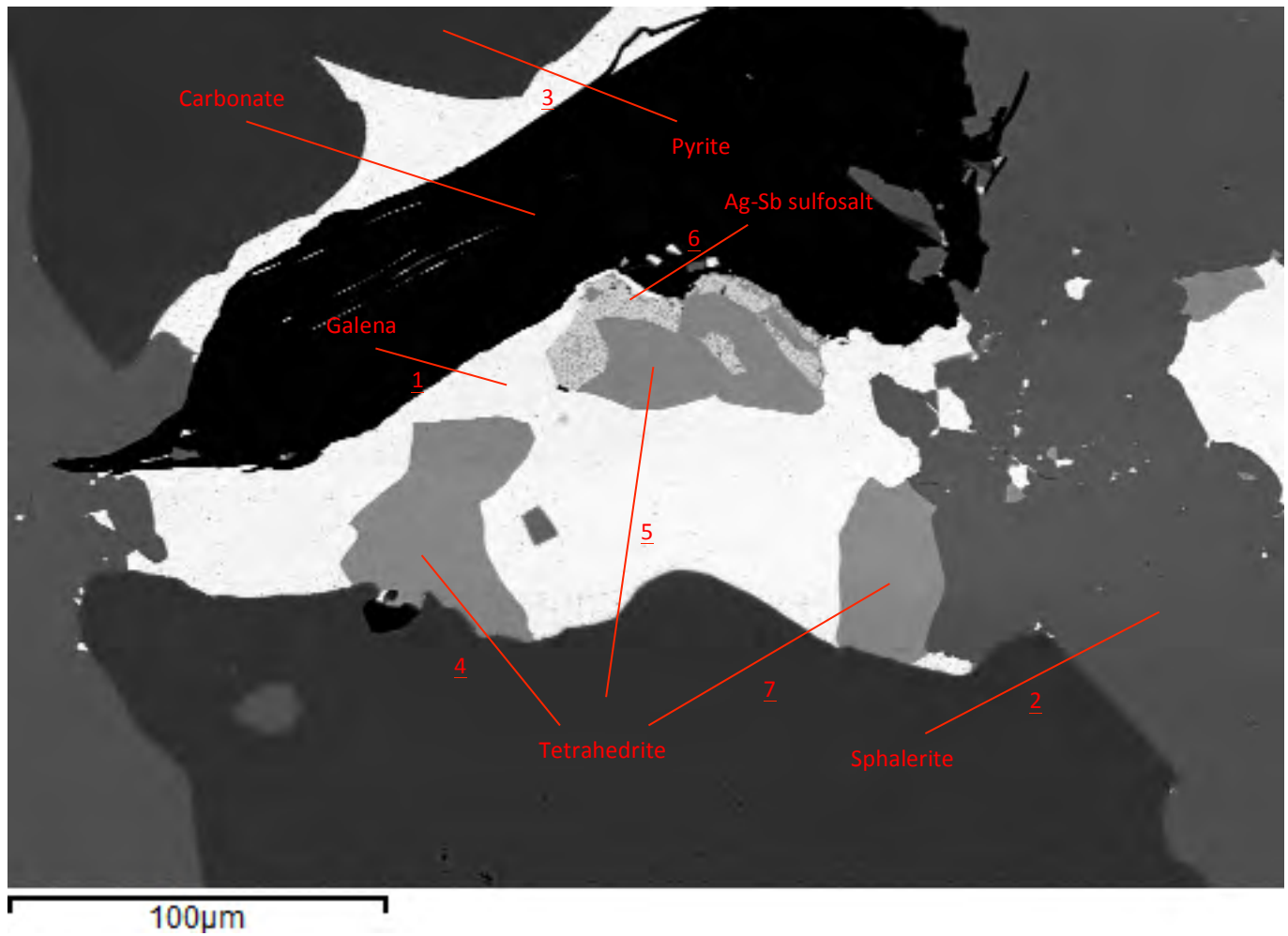


Fig.31. Photo showing area 2.

Spectrum	S (atomic %)	O	Fe	Cu	Zn	Pb	Ag	Sb	Ca	As	Hg	Mineral
1	52.40					47.60						Galena
2	53.82	3.18	3.75		39.24							Sphalerite
3	71.03		28.97									Pyrite
4	48.00		5.02	18.56	1.00		13.07	14.34				Tetrahedrite
5	48.07		5.10	19.22	1.37		12.06	14.18				Tetrahedrite
6	3.32	46.97		1.19			35.81	11.22			1.49	Ag-Sb sulfosalt
7	45.49	5.53	5.05	18.48	0.77		11.27	13.41				Tetrahedrite

Discussion

One of the most important purposes of this study was to determine the paragenesis of ore minerals in drill core 2559 by looking at the textural relationships between the different minerals. The paragenesis is the sequence in which the ore minerals form and evolve during the active life of the ore deposit. There are many textural relationships that help constrain the paragenesis such as inclusions of one mineral within another, replacement textures and cross cutting relationships between minerals and shared grain boundaries.

The paragenetic sequence for ore minerals investigated in this study is shown in figure 32. Most of the pyrite is clearly early with euhedral to subhedral pyrite being replaced by a later mineral such as pyrrhotite (Fig. 14), sphalerite (Figs. 15 and 16), galena (Fig. 17) and chalcopyrite. There are also several examples of pyrite being replaced by sphalerite creating the “caries” texture (Fig.8) where the replacing mineral forms a cavity in the earlier mineral. Some of the pyrite and arsenopyrite has very fine grain size which may indicate recrystallization during the paragenesis. Arsenopyrite is also interpreted to be early as it is commonly surrounded by the other phases and in places shows replacement by chalcopyrite, sphalerite, and pyrrhotite (Fig.33). Arsenopyrite often occurs together with pyrite indicating that they formed at the same time.

Sphalerite and galena are clearly spatially related with the galena occurring most commonly as patches within the sphalerite. There are no cross-cutting relationships between these two minerals and their textural relationship suggests they formed at the same time. Tetrahedrite almost always occurs within galena indicating that all three minerals formed during the same phase.

At least two different textures of pyrrhotite were identified. This mineral can occur as patches and commonly as needle-shaped inclusions within sphalerite (Figs. 7, 13, 14, and 18). This generation shows not cross-cutting relationships with the sphalerite and so is interpreted as being coeval. Pyrrhotite also occur as patches and as seen in (Fig.15) they occur along the rim of the mass of sulphides which means it formed during the late stages of paragenesis. Pyrrhotite also occurs in pressure shadows in deformed pumice bearing volcanigenic sedimentary samples (Fig. 21) indicating that it also formed very late in the paragenetic sequence during metamorphism and deformation.

Chalcopyrite occurs as patches within sphalerite and galena (Figs. 11 and 17) which suggests that at least some of the chalcopyrite formed at the same time as these minerals. However some of the chalcopyrite appears to invade and surround the sphalerite and galena indicating it may have continued to form later in the sequence.

The sulfosalts have formed through alteration of tetrahedrite and must therefore have formed after tetrahedrite and all other minerals that formed before or at the same time. Most likely the sulfosalts formed at the same time as the late chalcopyrite and pyrrhotite. Chalcopyrite is commonly present proximal to sulfosalts and is possibly a product of the alteration of tetrahedrite. It's almost impossible to determine where the ilmenite and titanite fits in the paragenesis since they don't share grain boundaries with any other ore

minerals so they have been left out of the paragenesis table shown in (Fig.32).

The degree of deformation in the core varies from sample to sample. Some samples like RS085 shows signs of significant deformation where mylonitic textures can be seen where minerals have smaller grains sizes because of shearing. Other samples like RS077 show very little signs of deformation which has allowed chlorite to develop fan texture (Fig.19). Deformation is very clear on the outside of the ore zone but less clear inside. This may be because the sulphide has fully recrystallized in response to deformation and metamorphism. Deformation and metamorphism likely occurred relatively late in the paragenesis since all ore minerals show signs of deformation and many minerals show signs of recrystallization. The remobilization may have been caused by melting since recent studies has shown that ore minerals can melt at temperatures achieved during amphibolite facies metamorphism but no clear evidence of this was found in this study (Tomkins. 2007). The sulfosalts and late pyrrhotite likely formed during deformation and metamorphism.

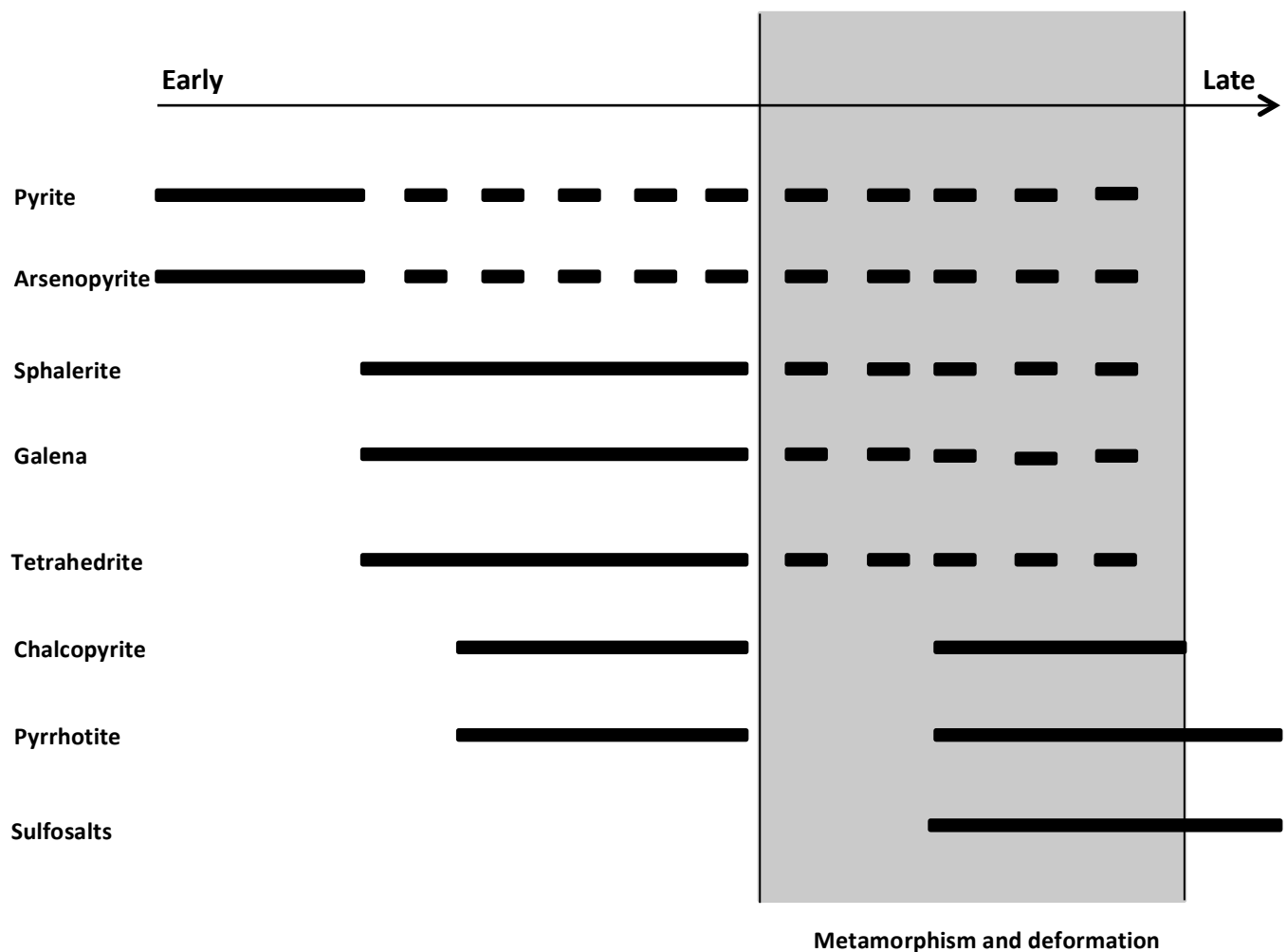


Fig.32. Table showing the paragenetic sequence of the ore minerals as well as the probable timing of deformation and metamorphism. Full lines indicate formation dotted lines indicate recrystallization.

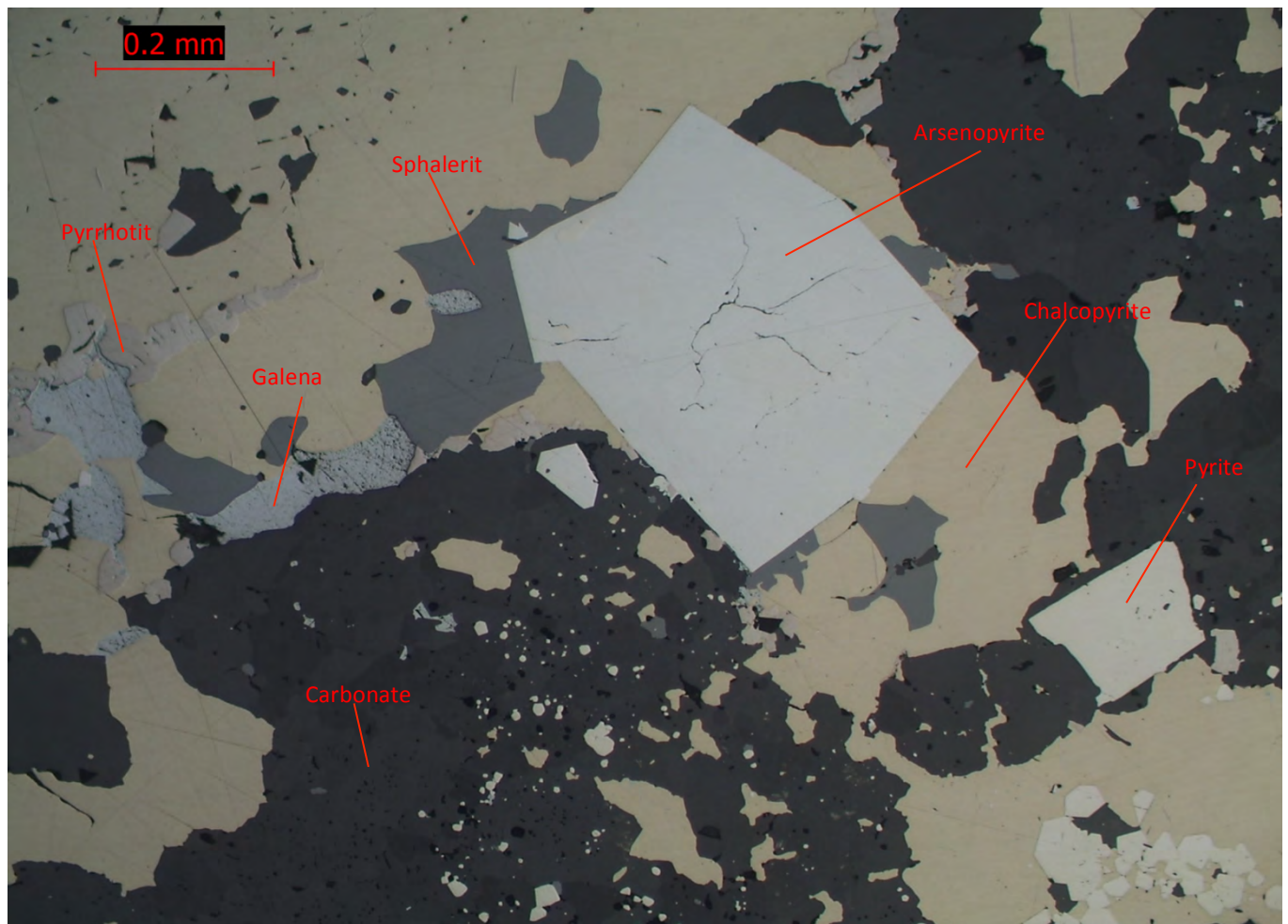


Fig.33. Arsenopyrite surrounded by sphalerite, chalcopyrite, pyrrhotite and carbonate.

Conclusion

Drill core 2559 has been variably deformed and has undergone greenschist facies metamorphism that has altered the mineralogy through remobilization. The paragenesis of the ore minerals started with the formation of pyrite and arsenopyrite. Sphalerite, galena and tetrahedrite formed during the next phase and after that the first stage of chalcopyrite and pyrrhotite formed. The minerals were then remobilized through metamorphism and deformation caused by shearing. During the last mineral phase late stage chalcopyrite and pyrrhotite formed as well as various Ag-Sb sulfosalts. The outside of the ore zone which consists mostly of host rock seem to be the most deformed while the inside of the ore zone is less affected. This is most likely because the sulphide was recrystallized in response to deformation and metamorphism.

Acknowledgements

I would like to thank my supervisor Iain Pitcairn for all the feedback he's given me and for having the patience to always answer any questions I might have. I would also like to thank Felix Makowsky for providing me with information about core 2559 whenever I needed it.

References

- Allen, R.L., Weihed, P., Svenson, S.Å. (1997). Setting of Zn-Cu-Au-Ag Massive Sulfide Deposits in the Evolution and Facies Architecture of a 1.9 Ga Marine Volcanic Arc, Skellefte District, Sweden. *Economic Geology*. 91 (6), p1022-1053.
- Allen, R. L., Svenson, S.-Å., 2004. 1.9 Ga Volcanic Stratigraphy, Structure, and Zn-Pb-Cu-Au-Ag Massive Sulfide Deposits of the Renström Area, Skellefte District, Sweden. *Society of Economic Geologists Guidebook*, Volume 33, pp. 65-88.
- Duckworth, R.C., Rickard, D. (1993). Sulphide mylonites from the Renström VMS deposit, Northern Sweden. *Mineralogical Magazine*. 57 (386), p83-91.
- Galley, A., Hannington, M., Jonasson, I. (2010). Mineral Deposits of Canada A Synthesis of Major Deposit-Types, District Metallogeny, the Evolution of Geological Provinces, and Exploration Methods. *Geological Survey of Canada*. 1 (1), p141-162.
- Tomkins, A.G. (2007). Three mechanisms of ore re-mobilisation during amphibolite facies metamorphism at the Montauban Zn–Pb–Au–Ag deposit. *Miner Deposita*. 42 (6), p627-637.
- Vernon-Parry, K.D. (2000). Scanning Electron Microscopy: an introduction. *III-Vs Review*. 13 (4), 40-44.
- Weihed, P., Arndt, N., Billström, K., Duchesne, J-C., Eilu, P., Martinsson, O., Papunen, H., Lahtinen, R. (2005). 8: Precambrian geodynamics and ore formation: The Fennoscandian Shield. *Ore Geology Reviews*. 27 (1-4), p273-322.